

Catalysis Science & Technology

Accepted Manuscript



This is an *Accepted Manuscript*, which has been through the Royal Society of Chemistry peer review process and has been accepted for publication.

Accepted Manuscripts are published online shortly after acceptance, before technical editing, formatting and proof reading. Using this free service, authors can make their results available to the community, in citable form, before we publish the edited article. We will replace this *Accepted Manuscript* with the edited and formatted *Advance Article* as soon as it is available.

You can find more information about *Accepted Manuscripts* in the [Information for Authors](#).

Please note that technical editing may introduce minor changes to the text and/or graphics, which may alter content. The journal's standard [Terms & Conditions](#) and the [Ethical guidelines](#) still apply. In no event shall the Royal Society of Chemistry be held responsible for any errors or omissions in this *Accepted Manuscript* or any consequences arising from the use of any information it contains.

MINIREVIEW

Earth-Abundant Metal Complexes as Catalysts for Water Oxidation; Is it Homogeneous or Heterogeneous?

Cite this: DOI: 10.1039/x0xx00000x

Received 00th January 2012,
Accepted 00th January 2012

DOI: 10.1039/x0xx00000x

www.rsc.org/

Md. Ali Asraf^{a,b,e}, Hussein A. Younus^{a,b}, Mekhman Yusubov^c, and Francis Verpoort^{a,b,c,d}

Recent developments in the oxidation of water to dioxygen using metal complexes as catalysts or precatalysts are represented at the side of the conversion of homogeneous catalysts into nanoparticles or heterogeneous one during the oxidation reaction of water. Homogeneous catalysts are advantageous within the careful design and elucidation of the mechanisms for the catalytic water oxidation. In distinction, the uses of heterogeneous catalysts in water oxidation are advantageous for sensible applications as a result of their robust catalytic activity. Though detailed studies on homogeneous and heterogeneous water oxidation reactions are performed rather severally, the connection of homogeneous catalysts with heterogeneous one is changing into an additional requirement for the event of economic attractive water oxidation catalysts (WOCs). This minireview focuses on the aspects if the particular catalysts for the oxidation of water are homogeneous or heterogeneous.

1. Introduction:

To meet the worldwide energy consumption and avoid potential environmental and nuclear disasters it is a key challenge for scientists to develop a sustainable and carbon-neutral energy. Therefore, scientists are looking for clean and sustainable energy resources supporting alternative energy are turning into far more vital. In depth, efforts to this point have been dedicated to develop a synthetic route of photosynthesis for sustainable fuel production.¹⁻¹⁴

^a Laboratory of Organometallics, Catalysis and Ordered Materials, State Key Laboratory of Advanced Technology for Materials Synthesis and Processing, Wuhan University of Technology, Wuhan 430070, China. E-mail: Francis@whut.edu.cn / Francis.verpoort@ugent.be, Tel.: +86 18701743583; Fax: +86 2787879468,

^b Department of Chemistry, Chemical Engineering and Life Sciences, Wuhan University of Technology, Wuhan 430070, China.

^c National Research Tomsk Polytechnic University, Lenin Avenue 30, 634050 Tomsk, Russian Federation.

^d Ghent University, Global Campus Songdo, 119 Songdomunhwa-Ro, Yeonsu-Gu, Incheon, Korea.

^e Department of Chemistry, Rajshahi University, Rajshahi-6205, Bangladesh.

There are numerous steps such as light harvesting, charge separation, catalytic processes for water oxidation, and reduction as well as carbon dioxide fixation of artificial photosynthesis. Currently, there are plenty of glorious synthetic systems mimicking functions of light harvesting and charge separation within the center of the photosynthetic reaction.¹⁵⁻²⁵ Earth-abundant metal oxide or hydroxide nanoparticles can act as robust catalysts for water reduction to hydrogen.²⁶⁻⁴¹ CO₂ fixation by hydrogen has conjointly been created doable by exploitation of homogeneous catalysts under normal pressure of H₂ and carbon dioxide and at room temperature as well.⁴²⁻⁴⁶ The step of water oxidation is the bottleneck of artificial photosynthesis because it needs the removal of four protons and four electrons from the catalytic site. In nature, the compound that achieves water splitting in the photosynthesis process is the oxygen-evolving complex (OEC), which exists in photosystem II, is known to be manganese-oxo-calcium cluster.⁴⁷⁻⁵¹ In recent years, water oxidation catalysts (homogeneous and heterogeneous) have been studied elaborately. The main advantage of homogeneous water oxidation catalyst over heterogeneous one is the ability to examine the reaction mechanisms. Understanding the reaction mechanism and identification of the reactive intermediates will give the opportunity for precise catalyst design and also tuning of the active catalysts.⁵²⁻⁶⁷



Md. Ali Asraf (1980, Bangladesh) earned his Bachelor of Science degree in Chemistry from Rajshahi University, Bangladesh in 2002. He received his Master of Science degree in Inorg. Chem. in 2003 from the same University. Now, he is a PhD candidate under the supervision of Prof. Francis Verpoort at the Laboratory of Organometallics, Catalysis and Ordered Materials, State Key Laboratory of Advanced Technology for Materials Synthesis and Processing, Wuhan University of Technology, China. His current research interests include catalysis, coordination chemistry, and water splitting.



Hussein A. Younus (1985, Egypt) received bachelor degree with distinction (2006) from Fayoum University, Egypt. He received his M.Sc. degree (2011) from the same university. At present he is PhD candidate under the supervision of Prof. Francis Verpoort at the Laboratory of Organometallics, Catalysis and Ordered Materials, State Key Laboratory of Advanced Technology for Materials Synthesis and Processing, Wuhan University of

Technology, China. His current research interests are focused on catalysis, metal complexes, metal-organic materials, and water splitting.



Mekhman S. Yusubov (Republic of Georgia) His M.S. (1985), Ph.D. (1991), and Doctor of Chem. Sci.s (1998) degrees were earned at Tomsk Polytechnic University in the laboratory of Professor Victor D. Filimonov. He is Head of the Department of Technology of Organic Substances and Polymer Materials Tomsk Polytechnic University and Head of the

Chemistry Department at the Siberian State Medical University. Since 1994 he has been involved in extensive international collaborative research programs with leading research laboratories in South Korea, Germany, the UK and USA. His main research interests are chemistry of hypervalent iodine reagents, polymer materials based on DCPD.



Francis Verpoort (1963, Belgium) received his DPhil from Ghent University in 1996. In 1998, he became a full professor at the same university. In 2004, he founded a spin-off company of Ghent University based on (latent) ruthenium olefin metathesis catalysts. In 2008, he became an Editor of Applied Organometallic Chemistry. Currently, next to Full Professor at Ghent University, he is a chair professor at

the State Key Laboratory of Advanced Technology for Material Synthesis and Processing (Wuhan University of Technology) and Director of the Center for Chemical and Material Engineering (Wuhan University of Technology). Recently, he has been

appointed as ‘‘Expert of the State’’ in the frame of ‘‘Thousand Talents’’ program, PR China. His main research interests concern the structure and mechanisms in organometallic material chemistry, homogeneous and heterogeneous catalysts, MOFs, water splitting, olefin metathesis and its applications, CO₂ conversion, and inorganic and organic polymers.

According to Oswald’s original definitions of homogeneous and heterogeneous catalysis, homogeneous catalysis is one where catalyst and substrate exists in the same phase (i.e. solution) and heterogeneous catalysis is one where catalyst and substrate exists in different phases.⁶⁸ In 1994, Yin Lin and R. G. Finke first disclosed a general method to identify the true catalyst (homogeneous or heterogeneous) in the hydrogenation reaction.⁶⁹ The same research group has also discussed the problems of the identification of the real catalysts whether the catalyst is a homogeneous metal complex or heterogeneous nanoparticles.⁷⁰ Antoni Llobet and his co-workers have discussed about the developments and challenges of water oxidation with molecular catalysts.⁷¹ Metal complexes supported with organic ligands might act as homogeneous catalysts or serve only as precursors of more active heterogeneous catalysts in water oxidation reaction.⁷² Crabtree conjointly mentioned in his in-depth article about the homogeneous and heterogeneous catalysis in various catalytic oxidation reactions.⁷³ Bonnet *et al.* discussed the stability of the catalysts in different oxidation reaction conditions and also the experimental studies of the expected decomposition pathways for water oxidation catalysts.⁷⁴ Polyoxometalates (POMs) are efficient water oxidation catalysts however they can be converted into nanoparticles or heterogeneous catalysts depending on the different oxidation reaction conditions. Finke and Stracke recently reviewed the frequently used experimental methods for the identification of the real catalyst (homogeneous or heterogeneous) for water oxidation reaction catalysed by polyoxometalates and also by non- polyoxometalates.⁷⁵ They proposed a stepwise protocol to differentiate homogeneous and heterogeneous catalysts, which consists of five basic steps: (1) Numerous experiments are required to determine the actual catalyst, through studying the catalyst stability and kinetics under operating conditions. (2) Control experiments using hypothetical expected heterogeneous catalysts such as metal-oxide or metal oxide nanoparticles are required to determine their kinetic competence in the reaction and support the conclusion whether the catalyst is homogeneous or heterogeneous. (3) The necessity of quantitative stability studies of the catalyst under reaction conditions, as the lack of this information makes it difficult to rule out the possibility of an alternative species as the true catalyst. (4) The stability of POMs is dependent on the polyoxometalate, the metal center, and the reaction conditions as well. (5) As a result of the variable stability of POMs under different reaction conditions, those different conditions might affect the dominant catalyst identity. A review based on POM catalysts for water oxidation reaction already has been published and there for POM catalysts are not included in this review. In addition, Fukuzumi and Hong discussed the factors by which homogeneous catalysts are converted into heterogeneous catalysts during water oxidation reaction.⁷⁶ In recent years, determination of the real catalysts for the oxidation of water to dioxygen has become an additional task for scientists working in the field

because extra cautions need to be taken to investigate research mechanics and to discover intermediates for the metal complexes if nanoparticles are produced from the homogeneous metal complexes throughout the oxidation reactions and acted as true catalysts. Hence, this minireview mainly deals with the link between homogeneous and heterogeneous metal catalysts and significantly focuses on the factors of water oxidation reaction in which molecular metal complexes are converted into metal oxide or hydroxide nanoparticles that act as robust water oxidation catalysts, providing important ways for the determination of the real catalysts and strategies to design additional economical water oxidation catalysts.

2. Molecular Cobalt Complexes for Homogeneous Water Oxidation:

It is still a vital challenge for scientists to develop efficient water oxidation catalysts (WOCs) using earth-abundant metals. WOCs supported earth-abundant metals are extremely desired for sensible applications. There are just a few catalysts based on cobalt complexes that can act as homogeneous WOCs.

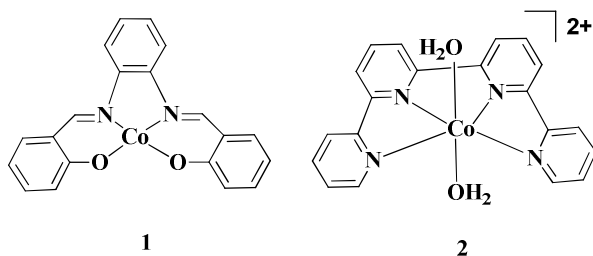


Figure 1 Structure of molecular cobalt complexes working as homogeneous WOCs.

Pizzolato *et al.* prepared cobalt (II)-salophen complex, CoSlp **1** (Figure 1), which was an active catalyst to perform the water oxidation reaction. They checked the catalytic activity of the catalyst for photochemical water oxidation reaction using persulfate ($S_2O_8^{2-}$) as the sacrificial electron acceptor and $Ru(bpy)_3^{2+}$ as the photosensitizer (PS) in neutral pH.⁷⁷ This complex was also able to catalyse the water oxidation to dioxygen in an electrochemical system. Under the catalytic reaction conditions, the quantum yield (ϕ_{O_2}) was found in the range of 0.048-0.079, which is equivalent to 9.6-15.8% efficiency in photon to O_2 conversion. The absorption spectra of CoSlp **1** in aqueous phosphate buffer (20 mM and pH 7) in the presence of $S_2O_8^{2-}$ for several hours showed no change, indicating that CoSlp **1** was stable under these reaction conditions. Moreover, DLS (dynamic light scattering) measurement of the reaction mixture under photochemical reaction conditions confirmed that no cobalt oxide or hydroxide nanoparticles were formed during water oxidation. Furthermore, the EPR spectrum of the catalyst did not demonstrate any changes even after illumination in the presence of PS and sacrificial electron acceptor. There were no peaks responsible for free Co (II) or Co (III) ions and thus, it was confirmed that the cobalt-salophen catalyst for water oxidation was stable and homogeneous under reaction conditions.

A quaterpyridine cobalt complex **2** also worked as homogeneous catalyst for photochemical and chemical water oxidation

reaction.⁷⁸ They examined the catalyst for photochemical water oxidation in borate buffer (pH 8) using $[Ru(bpy)_3]Cl_2$ as photosensitizer and $S_2O_8^{2-}$ as sacrificial electron acceptor while for the chemical water oxidation $[Ru(bpy)_3]^{3+}$ was applied as oxidant. The photocatalysis showed a low efficiency at $pH < 8$. Maximum turnover numbers of 335 for photochemical water oxidation and 160 ± 10 for chemical water oxidation were achieved respectively. The ESI-MS spectra of the reaction mixture after catalysis exhibited the peaks for $[Ru(bpy)_3]^{2+}$, $[Co(qpy)Cl]^+$, $Co(qpy)Cl_2^+$ and $[Ru(bpy)_3Cl]^+$. No other peak for free Co^{II} and qpy ligand in the MS spectrum was detected. DLS analysis showed no evidence of nanoparticles formation during water oxidation. Mass spectroscopy of the reaction mixture revealed that the catalyst was stable under the photochemical reaction conditions with negligible decomposition ($< 1\%$). With increasing catalyst concentration, both the turnover frequency (TOF) and turnover numbers (TON) were improved although the TOF was not really affected by the photosensitizer (PS) concentration. However, an optimum concentration of PS was noted. Similar effects of the sacrificial oxidant $Na_2S_2O_8$ were also pointed out.

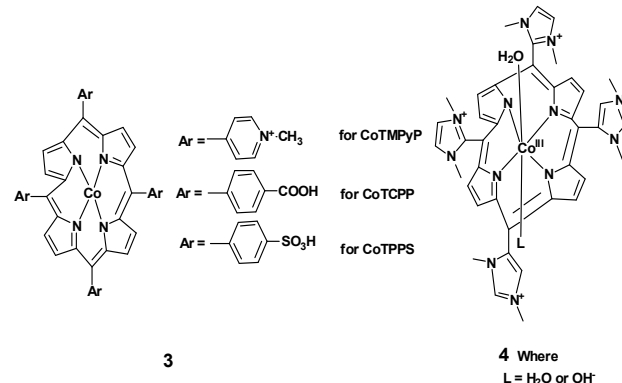


Figure 2 Cobalt porphyrin complexes acted as homogeneous WOCs

In 2013, Sakai and co-workers reported the O_2 -evolving activity of three cobalt porphyrin complexes **3** (Figure 2) driven by the $Ru^{III}(bpy)_3^{2+}/S_2O_8^{2-}$ system under basic conditions.⁷⁹ The turnover numbers after 30 minutes of CoTPPS, CoTCPP and CoTMPyP were 121.8, 103.4 and 88.7 respectively at pH 11. Dynamic light scattering (DLS) data confirmed that no nanoparticles were formed during the course of photocatalysis with porphyrin solution. Although $Co(bpy)_3^{2+}$ solution produced nanoparticles under the same reaction conditions (Figure 3). Though there was no evidence of the formation of nanoparticles, the efficiency of the catalyst, CoTPPS decreased with the addition of fresh $Na_2S_2O_8$ in the subsequent runs. For this, they concluded that the catalyst, CoTPPS converted or decomposed into other less catalytically active species, keeping the central metal ion cobalt ligated.

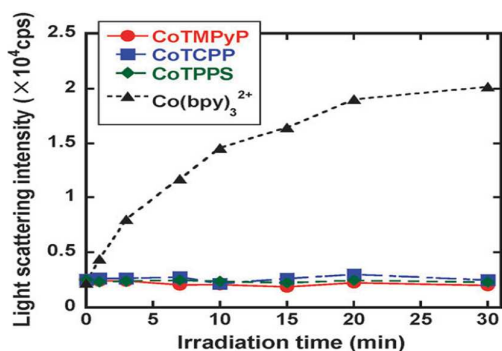


Figure 3 Light-scattering intensity as a function of time during illumination of 10 mM aqueous solution of **3** containing 1mM PS and 5.0mM $S_2O_8^{2-}$ in phosphate buffer (0.1mM, pH 11) under Ar.

Furthermore, stop-flow experiments confirmed that the initially observed water oxidation activity was attributable to initial Co(III) porphyrin species. Addition of concentrated HCl to the reaction mixture, obtained after photochemical water oxidation, resulted in the precipitation of the decomposition products. Characterization by ESI-MS confirmed oxidative cleavage of the porphyrin ring at the meso-positions. Notably, the resulting oxidation products appear to remain bound to the Co-ion, consistent with the lack of nanoparticle formation in this system.

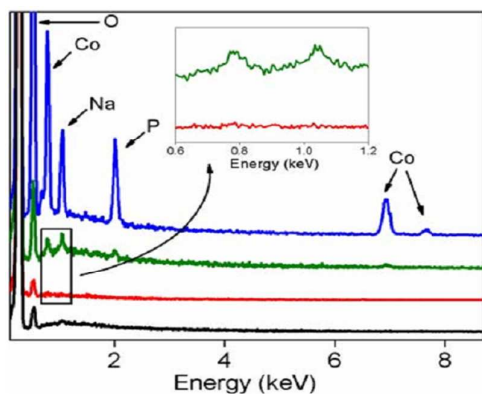


Figure 4 EDX measurement of freshly polished glassy carbon electrode (black); glassy carbon electrode after 20 CV scans in phosphate buffer solution (0.2 mM, pH 7) containing 5 mM **4** (red) and a cobalt oxide film on the surface of glassy carbon electrode after 20 CV scans in same phosphate buffer solution containing 1 mM (blue) and 0.1 mM $Co(NO_3)_2$ (green).

The cationic cobalt porphyrin, Co^{III} -TDMImP **4** catalysed electrochemical oxidation of water to O_2 in neutral aqueous media.⁸⁰ This system showed a Faradaic efficiency close to 90%. A maximum catalytic current was observed in the cyclic voltammogram (CV) of 1mM Co^{III} -TDMImP in 0.2mM phosphate buffer (pH-7) with the onset potential of *ca.* 1.2V. The O_2 formation from this system sustained for many hours while no significant loss of the current was observed and UV-Vis measurements throughout the electrolysis supported this. A variety of control experiments were carried out to know more about the formation of a metal oxide film during water oxidation. Q bands at 540 and 575 nm from the characteristic spectrum of the catalyst **4** confirmed that this catalyst did not decompose under operating conditions. Linear sweep voltammetry

additionally revealed that the chemical process activity of the catalyst remained stable over a period of 4 hours. Trials to exploit additives or reagents into the reaction medium that can scavenge any free Co^{2+} ions from the reaction mixture noted that there was no free Co^{2+} ion in the solution during catalysis. On the other hand, water oxidation activity of 0.2mM $Co(NO_3)_2$ was suppressed totally by the addition of 0.25 mM EDTA solution but did not effect on the catalytic activity of the catalyst **4**. The onset potentials obtained during the exploitation of Co-TDMImP and $Co(NO_3)_2$ and the shape of the chemical process waves were totally different. Once the operating electrodes were taken out from the catalyst solutions after multiple CV scans or bulk electrolysis and were utilized in fresh buffers, after slightly washing, no significant current was observed compared to the fresh electrodes. The surface of the working electrodes was examined by environmental scanning electron microscope (ESEM) and energy dispersive X-ray spectroscopy (EDX) after multiple CV scans in catalyst solution and showed very clean surfaces of the working electrode with no sign of any metal film but exhibited a metal film on electrode surface after CV scans in the same solution containing a very little amount of 0.1 mM $Co(NO_3)_2$ (Figure 4). The addition of Chelex beads in 0.2 mM $Co(NO_3)_2$ solution reduced the ascertained chemical process current drastically by sequestering of free Co^{2+} ions but had no impact on the ascertained catalytic current using catalyst **4** over the period of the experiment. On the other hand, the linear dependence of the chemical process current on the concentration of the catalyst suggested that Co-TDMImP was a single-site homogenous catalyst.

A mono cobalt aqua complex, **5** (Figure 5) with an oxidative stable pentadentate Py5 ligand $[Co(Py5)(OH_2)](ClO_4)_2$, [Py5 = 2, 6-bis(bis-2-pyridyl)methoxy-methane-pyridine], was able to drive electrochemical water oxidation in alkaline media in homogeneous conditions.⁸¹ Complex **5** was found to undergo a PCET step stabilizing a $[Co^{III}-OH]^{2+}$ unit, that further oxidizes to form a Co^{IV} intermediate that reacts with water in the presence of a base to produce O_2 . The water oxidation catalysis was indicated by the considerable rise in current at potential $> +1.2V$ vs. NHE relative to the $Co(III)/Co(II)$ proton coupled electron transfer step within the pH range of 7.6-10.3 (Figure 6). The overpotential of the water oxidation catalysis was 0.5 V (*e.g.* $E(H_2O/O_2) = +0.69V$ vs. NHE at pH of 9.2). From figure 6, it seems that this system leads to the deposition of a catalytically active film on the electrode surface as indicated by the increase in the wave current in the second cycle compared to the first cycle in the cyclic voltammogram scans. The authors subsequently performed cyclic voltammetry of $[Co(OH_2)_6](ClO_4)_2$ and $[Co(Py5)(OH_2)](ClO_4)_2$ **5**, using a glassy carbon working electrode. They claimed that a blue film was observed on the electrode surface after anodic cycling in the solution of $[Co(OH_2)_6](ClO_4)_2$ but no film was observed after anodic cycling in the solution of **5** (as mentioned in the manuscript ESI). However, the surface of the electrodes after CV using any techniques for post-electrolysis characterization such as SEM, XPS, *etc.* were not used, instead only naked-eye observations were mentioned. Additionally, no CV of a previously used GCE in a catalyst free buffer, as an easy tool to detect any film deposition, was presented.

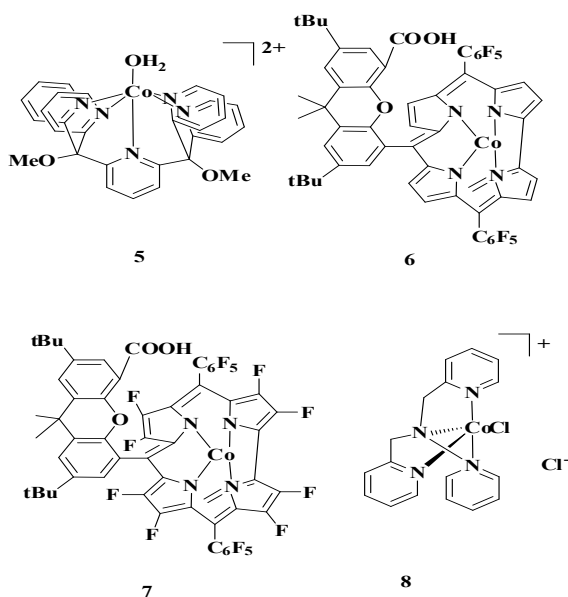


Figure 5 Molecular cobalt complexes for homogeneous water oxidation

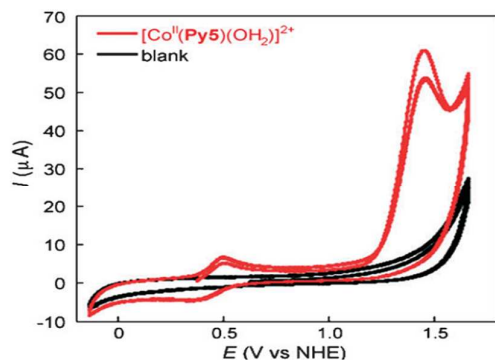


Figure 6 CV of **5** recorded in phosphate buffer solution (0.1 mM, pH 9.2) with scan rate of 50 mV/s (red) and a blank scan without **5** under the same conditions (black).

In 2010, Nocera and co-workers reported that Co(II) hangman porphyrin complex was in a position to perform $4e^-/4H^+$ reduction of O_2 into H_2O , the reverse reaction of water oxidation.⁸² Later, they synthesized Co (III) complexes **6** and **7** with β -octafluoro hangman corrole ligand. They modified the β -pyrrolic positions of the macrocycle by fluorination and by fluorinated phenyl groups as well.⁸³ Their ultimate goal was to improve the catalytic activity of the Co complex. Complex **7** showed catalytic oxidation of water at +1.25V vs. Ag/AgCl in neutral pH. UV-Visible, HRMS and LD-MS MALDI-TOF analysis confirmed that the catalyst **7** was stable or homogeneous during electrochemical oxidation of water to dioxygen. No CO_2 was detected in this system. The turnover frequency, TOF/Co atom of catalyst **7** was $0.81s^{-1}$.

A new cobalt(II) complex with the ligand TPA (TPA = tris(2-pyridylmethyl)amine), $[Co(TPA)Cl]Cl$ **8** acted as homogeneous catalyst for light-driven water oxidation where $[Ru(bpy)_3](ClO_4)_2$ and $S_2O_8^{2-}$ were used as photosensitizer and sacrificial electron acceptor respectively.⁸⁴ The TOF and TON were $1.0 \text{ mol } (O_2) \text{ mol.}(Co)^{-1}s^{-1}$ and $55 \text{ mol } (O_2) \text{ mol.}(Co)^{-1}$ in borate buffer (pH 8).

Once $[Ru(bpy)_3]Cl_2$ was used as PS rather than $[Ru(bpy)_3](ClO_4)_2$, the O_2 yield increased by a factor of 4. The authors carried out comparative water oxidation experiments using **8** and $Co(ClO_4)_2$ under the same reaction conditions to find out whether nanoparticles were formed in case of **8**. The system containing $Co(ClO_4)_2$, $[Ru(bpy)_3](ClO_4)_2$ and $S_2O_8^{2-}$ produced rapid O_2 evolution and after ceasing of the O_2 formation additional, PS and $S_2O_8^{2-}$ were added to this system. O_2 evolution restarted without addition of catalyst, suggesting that nanoparticles were formed during catalysis using this system. However, in case of **8**, after long time illumination, even with $100\mu M$ of **8**, no nanoparticles were observed. Consequently, this complex was the true catalyst for the water oxidation.

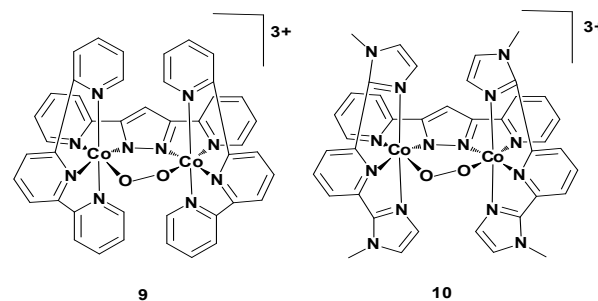


Figure 7 Dinuclear cobalt peroxo-bridged complexes for homogeneous water oxidation.

Dinuclear cobalt (III) peroxo complexes **9** and **10** worked also as homogeneous water oxidation catalysts.⁸⁵ Complexes **9** and **10** were capable to drive electrochemical water oxidation reaction at pH 2.1 (0.1M phosphate buffer) and were stable for several hours without decomposition to CoO_x nanoparticles. Complex **9** exhibited a first quasi-reversible wave at 1.56V vs NHE, ascribed to the $Co^{IV} Co^{III}/Co^{III} Co^{III}$ redox couple and a catalytic wave at 1.91V vs. NHE. Electrochemical measurements showed a second oxidation wave at 1.82V corresponding to the $Co^{IV} Co^{IV}/Co^{IV} Co^{III}$ redox couple, indicating that water oxidation occurred after reaching the $Co^{IV} Co^{IV}$ state. Complex **10** showed two redox waves at lower potential (1.35V and 1.84V vs. NHE) compared to **9**.

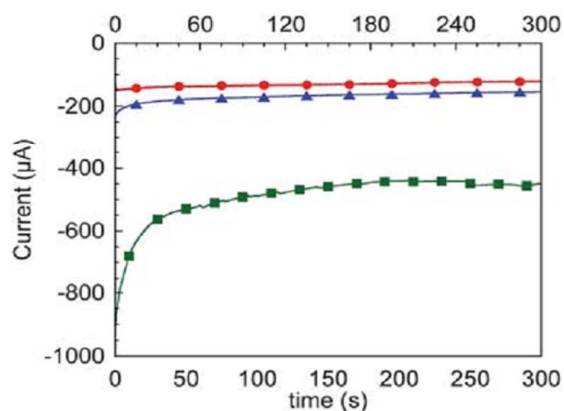


Figure 8 Controlled potential electrolysis of complex **9** (red), complex **10** (blue) and $CoSO_4$ (green) in 0.1M phosphate buffer (pH=2.1) at 2.0V; $[Analyte] = 0.25mM$.

Nanoparticles formation during the catalytic reaction was ruled out since nanoparticulate and heterogeneous CoO_x are not stable under acidic reaction conditions used in this experiment. Controlled potential electrolysis (CPE) measurements of complexes **9** and **10** (Figure 8) at 2.0 V showed a steady-state current over five hours of electrolysis. This behaviour confirmed that **9** and **10** act as true catalysts for the oxidation of H_2O to O_2 .

3. Molecular Cobalt Complexes Acting as Precatalysts or Heterogeneous WOCs:

Recently, cobalt complexes as catalysts for water oxidation reaction have gained more attention from scientists because cobalt is earth-abundant and inexpensive opposed to other noble metals. In addition, cobalt has the ability of self-preparing heterogeneous cobalt oxide or hydroxide nanoparticles with high WO activity.

Recently, Du and his co-workers developed a series of cobalt complexes which acted as precursor for electrocatalytic water oxidation.⁸⁶ Among the investigated complexes, complex **1** (Figure 1) exhibited a maximum water oxidation activity of 93% Faradaic efficiency at $\sim 350\text{mV}$ overpotential. Therefore, catalyst films were prepared on FTO electrodes using the complexes thereafter; FTO electrodes were invoked as working electrode for bulk electrolysis measurement in 0.1M KBr solution (pH 9.2) at 1.2V vs Ag/AgCl. The CV of complex **1** coated on FTO electrode at 1.5V vs Ag/AgCl revealed remarkable changes during CV scans, confirming the decomposition of **1** (Figure 10).

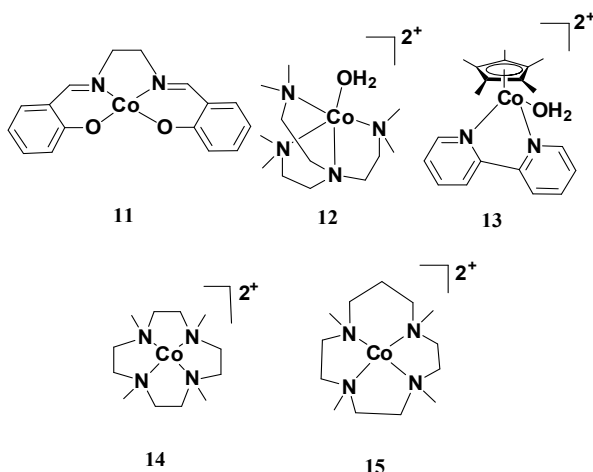


Figure 9 Cobalt complexes working as heterogeneous WOCs.

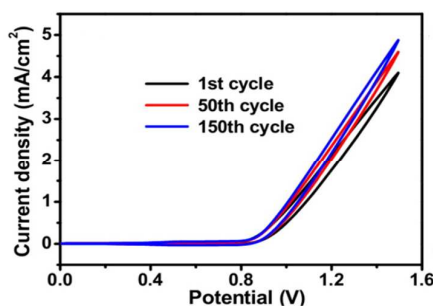


Figure 10 CV scans of **1** coated on FTO electrode from the first to 150th cycle.

A SEM image of the film deposited from complex **1** on FTO electrode after 11 hours of bulk electrolysis measurement in 0.1M borate buffer confirmed the formation of nanoparticles on the surface of the FTO electrode. EDX and XPS spectra confirmed the presence of Co and O in the deposited film. The high-resolution XPS spectrum of the Co 2p region disclosed the presence of Co(II) and Co(III) substances from the binding energies of Co 2p_{3/2} and Co 2p_{1/2} situated at 779.95 and 794.89 eV, respectively. The Tafel plot of the film exhibited a slope of $\sim 62\text{mV/decade}$, suggesting that the film deposited from **1** was strongly active for H_2O oxidation.

In 2014, Fu and co-workers reported that salen Co(II) complex **11** (Figure 9) acts as precatalyst for photochemical oxidation of water in borate buffer (pH 9) by using the $[\text{Ru}(\text{bpy})_3](\text{ClO}_4)_2/\text{S}_2\text{O}_8^{2-}$ system and a turnover number of 854 was obtained.⁸⁷ A 54.6% O_2 yield and 13.7 mmol O_2 evolutions was achieved in 80mM borate buffer at a pH of 9.0 for 1.6 mM of **11**. Three experiments were conducted to investigate the hydrolytic stability of **11**. An UV-Vis study showed that the catalyst was stable in buffer solution throughout the oxidation reaction and kinetics of O_2 formation contrast tests also demonstrated that complex **11** was stable in buffer solution. Finally, DLS experiment revealed that the complex was stable in buffer and no nanoparticles were produced even in the aging period. On the other hand, DLS measurements of the complex after illumination confirmed the formation of different sizes of particles during the reaction. The particles produced during the light-driven water oxidation by catalyst **11** were probably inorganic Co(III) species or mixture of $\text{Co}(\text{OH})_3$ or/and Co_2O_3 which was confirmed from the ESI/MS, XPS, and $^1\text{H-NMR}$ studies. Thus, ESI/MS analysis of the DCM extract of the photochemical WO experiment showed only peaks correlating to the photosensitizer, with neither detection of the complex **11** nor the free ligand or the cobalt aqua species.

The water-soluble mononuclear cobalt complexes, $[\text{Co}^{\text{II}}(\text{Me}_6\text{tren})(\text{OH}_2)]^{2+}$ **12**, $[\text{Co}^{\text{III}}\text{Cp}^*(\text{bpy})(\text{OH}_2)]^{2+}$ **13**, $[\text{Co}^{\text{II}}(12\text{-TMC})]^{2+}$ **14**, and $[\text{Co}^{\text{II}}(13\text{-TMC})]^{2+}$ **15** [Me_6tren = tris(N,N' -dimethylaminoethyl)-amine], [12-TMC=1,4,7,10-tetramethyl-1,4,7,10-tetraazacyclododecane, 13-TMC= 1,4,7,10-tetramethyl-1,4,7,10-tetraazacyclotridecane] (Figure 9) are another series of cobalt based precatalysts for light-driven oxidation of water.⁸⁸ The O_2 yield with $\text{Co}(\text{NO}_3)_2$, **12**, **13**, **14**, and **15** at pH 8.0 were 52, 54, 29, 16, and 41%, respectively. The O_2 yield was heavily dependent on the ligand environment and for catalysts **12** and **13** a quantum yield of 32 and 30% at pH 8.0 was obtained, respectively. Evolved O_2 was exclusively from water, which was confirmed from isotope-labelling experiments in which ^{18}O -enriched water was used instead of H_2^{16}O . About 20 nm sized nanoparticles were produced from the buffer solution of pH 9.0 containing **12** (50 μM), $[\text{Ru}(\text{bpy})_3]^{2+}$ (0.50 mM), and $\text{Na}_2\text{S}_2\text{O}_8$ (10 mM) after 3 mins photo-irradiation ($\lambda > 420\text{ nm}$) and the particle size did not change significantly up to 30 mins of photo-irradiation. However, particles size for the particles produced from complex **13** was in the range of 100 to 500 nm after 3 mins photo-irradiation and their size increased with the extension of irradiation time. Similar like the increasing in size from the particles derived from 50 μM solution of $\text{Co}(\text{NO}_3)_2$ when the photo-irradiation time was extended to 30 min. These studies confirmed that nanoparticles were formed from **12**, **13** and

Co(NO₃)₂ from the initial stage of the photo-irradiation. The X-ray photoelectron spectrum (XPS) of the standard Co₃O₄ sample was compared to the XPS spectrum of the particles derived from the complex **12**. The Co 2p_{1/2} and Co 2p_{3/2} peaks of the nanoparticles displayed weak satellite peaks at 780.0 and 795.3 eV, respectively. Co₃O₄ also showed two stronger peaks with feeble satellite peaks at 779.8 and 795.1 eV for Co 2p_{1/2} and Co 2p_{3/2}, respectively. The presence of such weak satellite peaks in the XPS spectrum indicated the existence of Co^{II} species. The O1s peak of the particles appeared at 531.5 eV and was shifted to a higher binding energy region compared with the same peak of Co₃O₄ (530.3 eV) (Figure 11). This binding energy increment of the O1s peak for the particles has been observed for M(OH)_x species. Therefore, this confirmed that the particles generated by **12** during light-driven oxidation of water were cobalt hydroxide species acting as the true catalyst. Complex **12** was converted into nanoparticles during oxidation reaction and was confirmed by ¹H-NMR analysis of the reaction mixture after illumination.

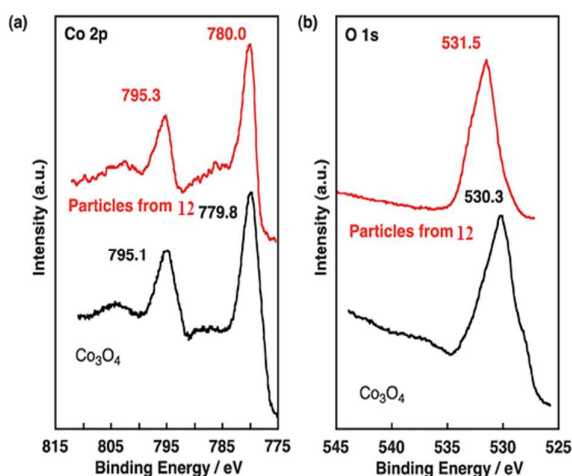


Figure 11 XPS spectra of the particles produced from the complex **12** (red) and Co₃O₄ (black) as a reference material in the energy regions of (a) Co 2p and (b) O 1s

It was reported that cobalt cubane compounds such as [Co₄O₄(OAc)₄(py)₄] and [Co^{III}₄(μ-O)₄(μ-OAc)₄(p-NC₅H₄X)₄], (where, X=H, Me, *t*-Bu, OMe, Br, COOCH₃, and CN) can catalyse water oxidation to O₂.^{89, 90} Although very recently, Noceras' research group prove that such types of cobalt cubane compounds were not catalytically active for the water oxidation reaction and the water oxidation activity of cobalt cubane-like compounds mainly arose from a Co(II) impurity in which the Co(II) impurity oxidized to form a heterogeneous WOC.⁹¹

From the above discussion on cobalt complexes as catalysts for homogeneous and heterogeneous water oxidation, it is very important to note that an unoccupied coordination site in the

central Co(II) atom of the complex can play a vital role for the oxidation of water. Cobalt complexes with organic ligands are very attractive candidates for scientists in the field of water oxidation since active Co(II) ions can be isolated on the atomic level. Furthermore, modification of the chemical structure of the ligands can control their activity to that limit they still remain stable under turnover conditions. Organic ligands usually decomposed under highly oxidative conditions. Hence, researchers should emphasize on the selection of the ligand (*e.g.* inorganic ligands) of cobalt complexes to obtain robust catalyst for water oxidation. Moreover, acidic conditions should stabilize the organic ligands against oxidative decomposition. There are some variables such as buffer types, pH, PS and catalyst concentrations that can affect the water oxidation activity of catalysts. Consequently, a systematic investigation is required to obtain optimal conditions for water oxidation catalysis. It is surely difficult to identify whether the catalytic activity originates from the starting molecular catalyst, from other secondary homogeneous complexes or even from heterogeneous nanocrystalline (cobalt oxide or hydroxide) decomposition products. From the above discussion it is clear that to determine the nature of catalytic species responsible for water oxidation, a complete set of characterization techniques must be carried out.

4. Fe Based Molecular Complexes for Homogeneous Water Oxidation:

Iron is without any doubt the foremost attention-grabbing metal to develop water oxidation catalysts. This metal is cheap, earth-abundant and very attractive for water oxidation reaction. The access to higher oxidation states encourages the use of iron-based complexes in a variety of redox reactions. Consequently, iron is strongly expected to be utilized in the building of artificial water oxidation catalysts. A few examples of Fe-complexes as homogeneous WOCs have been reported. Designing special ligand architectures that permit the generation and stabilization of high-valent iron species that are robust enough to allow H₂O oxidation to occur remains challenging.

Bernhards' research group investigated complexes **16-20** with substituents of varying electronic properties (Figure 12) as catalysts for chemical water oxidation in pH 0.7 using CAN (ceric ammonium nitrate).⁹² While the complex **16** was not active at all, probably because of its stability issue in acidic conditions, complexes **17-20** were active catalysts for water oxidation. Catalyst **20** showed the maximum turnover frequency (TOF > 4680 h⁻¹), highlighting the key role of the electronic properties of the ligands and that electron-withdrawing substituents increased the rate. Oxygen production was also pointed out when NaIO₄ was utilized as oxidant. Finally, they concluded from mechanistic studies that Fe(IV)-O-Fe(IV) was responsible for the oxidation of water to dioxygen.

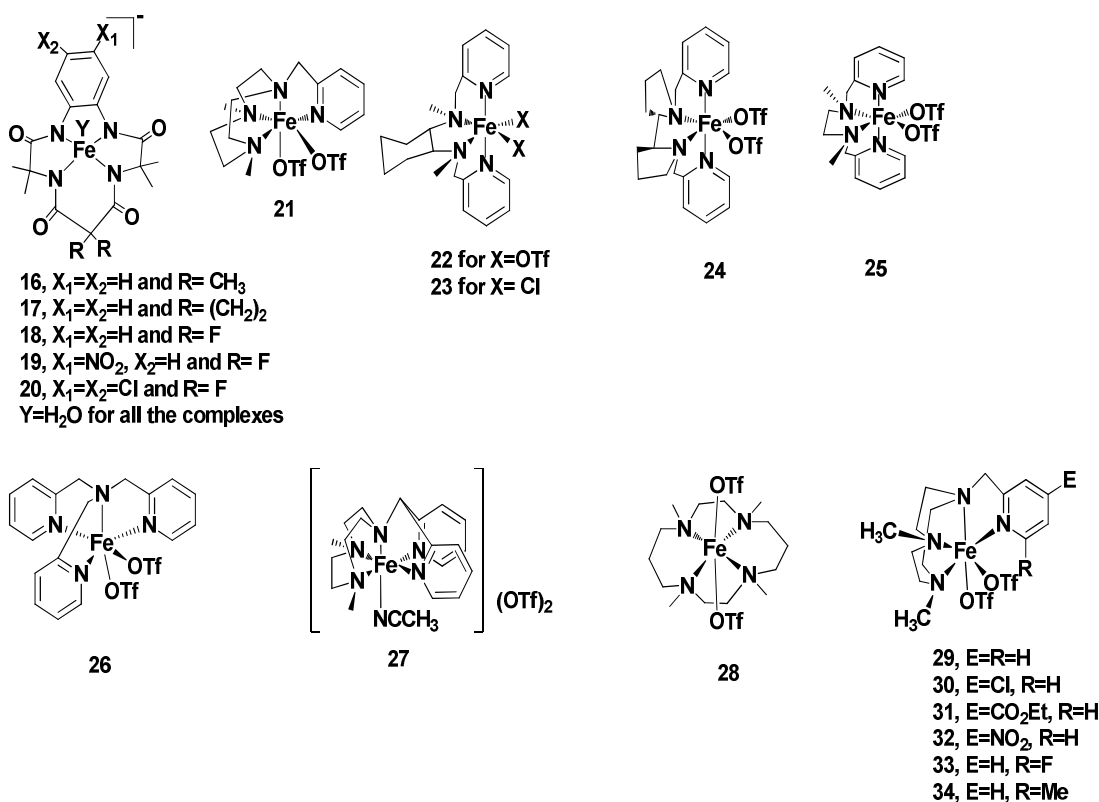


Figure 12 Structures of Fe-based homogeneous WOCs.

Moreover, control experiments using less complex iron precursors, such as oxide, nitrate, acetate of iron in the presence or absence of the TAL (tetraamido macrocyclic) ligand, resulted in no evolution of O_2 , confirming the unique reactivity of the Fe-TAM complexes.

Fillolet *al.* studied catalysts **21–28** for water oxidation using CAN and NaO_4 as oxidant and all of catalysts showed robust activity.⁹³ The maximum TON's (>1000) was observed with complex **22** and it is the highest TON's among the Fe-based homogeneous WOCs catalysts. Surprisingly, catalysts with *cis*-available coordination sites were active but the catalysts **27** and **28**, with *trans*-available coordination sites, were not active for the oxidation of water. Isotope labelling studies revealed that O_2 was formed from H_2O not from oxidants. A Fe(III)oxohydroxodiferric dimer as the main intermediate compound in this catalytic system was totally excluded due to its very low activity. The UV-Vis spectra ($\lambda_{max} = 776$) of the titration mixture of iron complexes with CAN confirmed that Fe(IV)=O species were responsible for the oxidation reaction. Under the same conditions, complexes **29–33** also showed catalytic activity in the following order **32** > **31** > **30** > **29** > **33** for water oxidation reaction with TON's in between 25 ± 3 and 180 ± 8 and TOF in between 80 ± 1 and 815 ± 69 .⁹⁴ Time courses analysis of water oxidation catalysis showed that robust

catalytic activity was observed when electron-withdrawing group (NO_2) is present at the *para*-position of the pyridine ligand as in complex **32**. Very low and no catalytic activity was observed when electron-withdrawing groups (F, CH_3) were present at the *ortho*-position of the pyridine ligand as in complexes **33** and **34**. Complex **32** was about two times more active and virtually fourfold faster than the antecedently reported catalyst **29**. The species **29-Fe^{IV}(O)** to **32-Fe^{IV}(O)** were formed during the titration of the complexes **29–32** with CAN which was suggested by the characteristic UV-Vis bands at a λ_{max} of 776, 778, 770, and 754, respectively. This chemical analysis was the confirmation for the formation of Fe^{IV} species $[Fe^{IV}(O)(OH_2)(L^{N4})]^{2+}$, **29-Fe^{IV}(O)** to **32-Fe^{IV}(O)**. Electrospray mass spectrographic analysis (ESI-MS) confirmed the formation of $[Fe^{IV}(O)(OH_2)(L^{N4})]^{2+}$ in solution. *In-situ* generated **29-Fe^{IV}(O)–32-Fe^{IV}(O)** had $t_{1/2} > 90$ min and for that, this oxidation state itself was not liable for the formation of O-O bond. Oxygen formation was observed by the addition of excess CAN to a solution of **29-Fe^{IV}(O)–32-Fe^{IV}(O)** and continued till complete consumption of Ce^{IV} , and therefore the quantitative relation of O_2 evolved/ Ce^{IV} consumed was more or less 1/4. Finally, the systematic study of the electronic effects on the water oxidation activity of the catalysts **29–32** firmly confirmed that these were homogeneous WOCs.

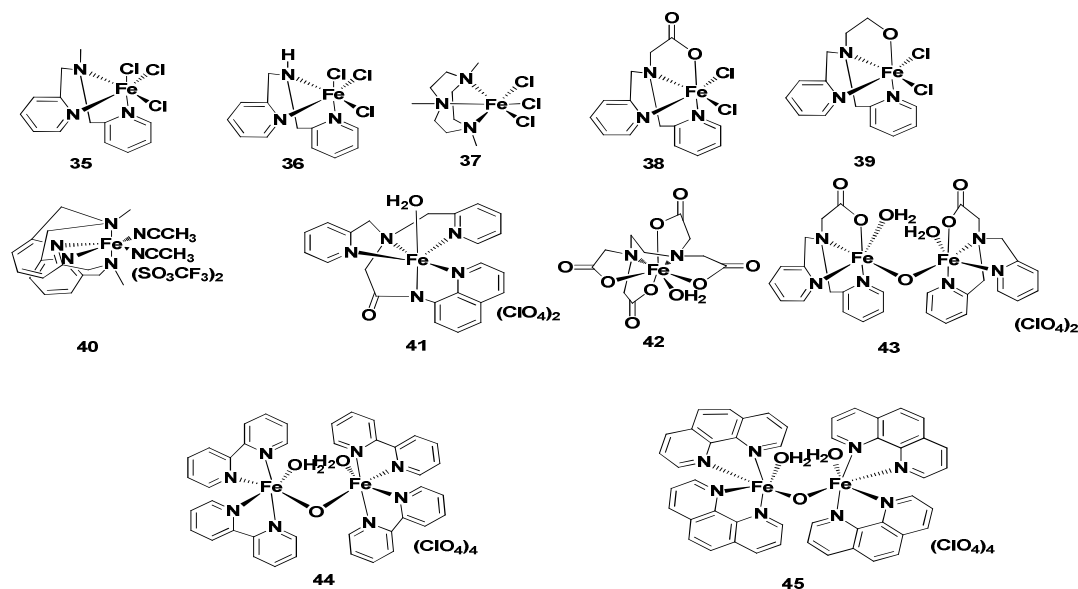


Figure 13 Iron complexes works as homogeneous WOCs.

The catalytic activity of a series of different Fe catalysts **35–45** and some others *in situ*-generated Fe catalysts for water oxidation reaction using the oxidant, CAN in aqueous $\text{CF}_3\text{SO}_3\text{H}$ solution (pH = 1) has been reported.⁹⁵ Only the catalysts **37** and **40** with macrocyclic ligands were active for the water oxidation reaction. Oxygen evolution rate was very small when the complex **37** was used as catalyst. Upon increasing the concentration of **37** from 4 μM to 120 μM , 400 μmol of O_2 were produced in 1 min and a TON of 1.6 was obtained. The use of the complex **40** led to better results where O_2 formation lasted for 40 min with a turnover numbers of 65. The *in-situ* generated Fe catalysts with the ligands such as 2, 6-pyridinedicarboxylic acid, imidazole, and 8-hydroxy quinoline were not active for water oxidation reaction. No metal oxides were found in this catalytic system because of strong acidic conditions. Therefore, the possibility of Fe^{3+} ions as catalytically active species in that system was further investigated but no O_2 was observed from FeCl_3 or $\text{Fe}(\text{NO}_3)_3$. Later on, UV-Vis spectral studies were performed by changing Fe catalysts in aqueous $\text{CF}_3\text{SO}_3\text{H}$ solution (pH = 1). This study disclosed that complexes **35**, **38**, **39**, and **43** quickly decomposed under the experimental conditions while complexes **37** and **45** decomposed at a slower rate. Complexes **36**, **40**, **41**, and **42** were stable during the period of measurement.

Meyer and co-workers reported that the hexa-coordinated Fe^{III} -complex, $[\text{Fe}^{\text{III}}(\text{dpaq})(\text{H}_2\text{O})](\text{ClO}_4)_2$ **46** (dpaq= 2-[bis(pyridine-2-ylmethyl)amino-N-quinolin-8-yl-acetamido], (Figure 14), was an active electrocatalyst for water oxidation in propylene carbonate with H_2O as a limiting chemical agent.⁹⁶ 29 μmol of O_2 were formed after 15h electrocatalysis at 1.58V vs. NHE and amounts to 45% Faradaic efficiency. Experimental results confirmed that the catalyst was stable and did not decompose in PC/ H_2O mixture under experimental conditions. In 2013, Fukuzumi *et al.* reported the photochemical and thermal water oxidation using non-heme Fe catalysts, $\text{Fe}(\text{BQEN})(\text{OTf})_2$ **47** and $\text{Fe}(\text{BQCN})(\text{OTf})_2$ **48** (where, BQEN= N,N'-dimethyl-N,N'-bis(8-quinolyl)-ethane-1,2-diamine, BQCN= N,N'-dimethyl-N,N'-bis(8-quinolyl)-cyclohexanediamine, and $\text{OTf} = \text{CF}_3\text{SO}_3^-$), with the aim to

disclose the real catalysts concerned in those chemical process systems.⁹⁷

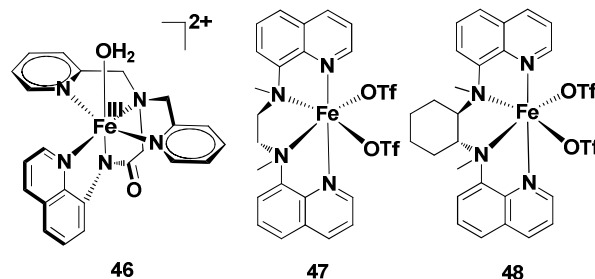


Figure 14 Structure of mononuclear iron complexes used in water oxidation reaction studied by Mayer and Fukuzumi research groups.

The catalysts **47** and **48** catalysed the oxidation of water homogeneously by CAN with ligand oxidation in acidic reaction conditions. On the other hand, they are converted into nanoparticles which were the real catalysts during photochemical water oxidation in basic reaction conditions. Thus, the natures of these two catalysts for water oxidation were different depending on experimental conditions such as pH, and the oxidizing agent. The TON's for the chemical water oxidation reaction by the catalysts **47** and **48** were 80 ± 10 and 20 ± 5 at 60 min, respectively. However, a small quantity of CO_2 was conjointly evolved during the oxidation process. The quantity of CO_2 evolution ascertained with **48** was 4.1 μmol at 60 min and it was *ca.* three times greater than the amount ascertained with **47** (1.4 μmol), suggesting that the ligand BQCN was easily oxidizable by the oxidant, CAN. Based on DLS measurements (Figure 15), no formation of nanoparticles was discovered during chemical water oxidation reaction, most probably due to the instability of iron oxides under these strongly acidic operating conditions and instead it does exist as $\text{Fe}(\text{III})$ ions. The $\text{Fe}^{\text{IV}}=\text{O}$ species produced from the oxidation of the catalysts by CAN in acid media were concerned within the oxidation reaction of water.

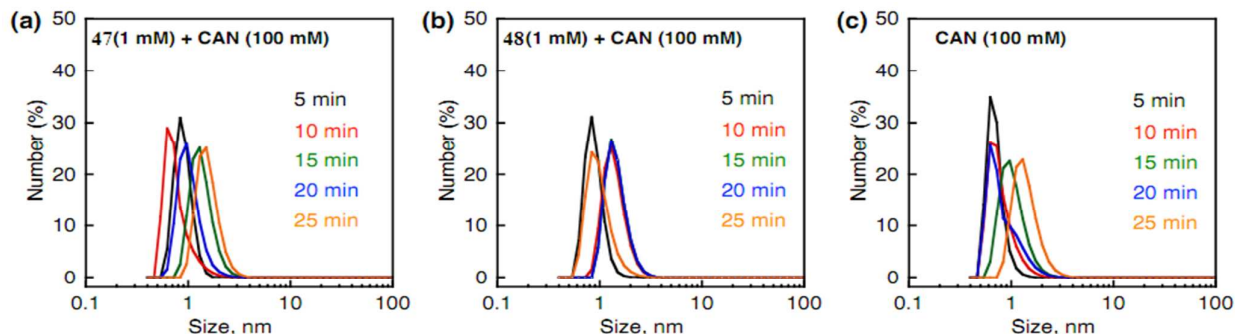


Figure 15 Particle size distribution examined by DLS analysis of non-buffered aqueous solutions of (a) 1.0 mM of **47** with 0.1M CAN, (b) 1.0 mM of **48** with 0.1M CAN, and (c) 0.1M CAN only at reaction times of 5.0 min (black), 10 min (red), 15 min (green), 20 min (blue), and 25 min (orange).

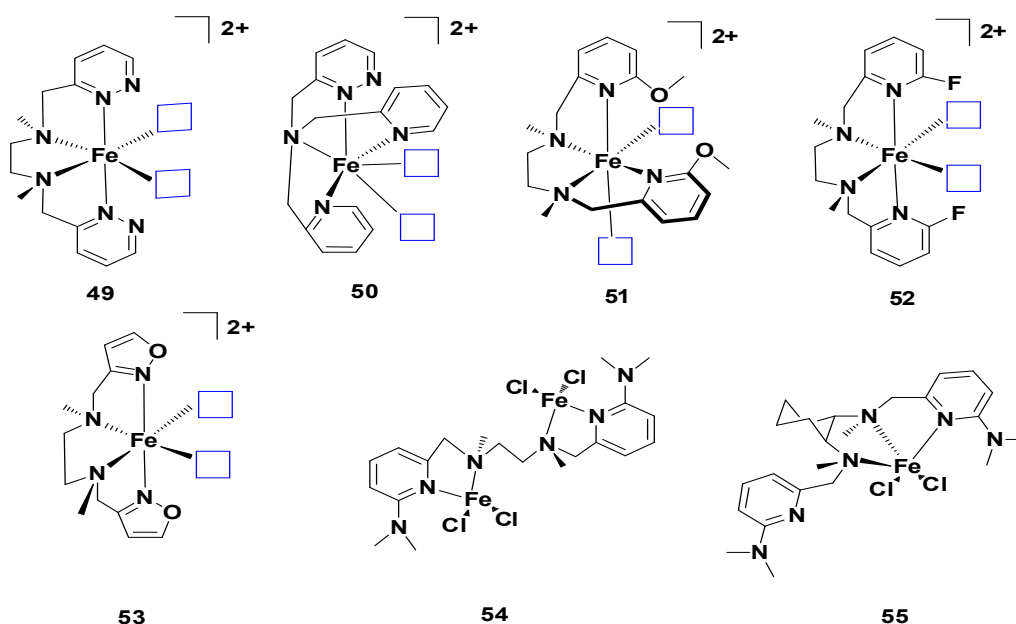


Figure 16 Structural representations of the synthesized Fe^{II} complexes (Blue boxes represents the labile coordination sites that are filled by either anionic ligands or solvent molecules).

Recently, Hoffert and his co-workers reported on the catalytic activities of the complexes **49-55** (Figure 16) with pendant bases for homogeneous water oxidation.⁹⁸ Among these new complexes, **49** $[\text{Fe}(\text{L}^1)]^{2+}$ [$\text{L}^1 = \text{N,N}'\text{-dimethyl-N,N}'\text{-bis(pyridazin-3-yl-methyl)ethane-1,2-diamine}$] was the foremost robust catalyst. The initial TOF of 141 and 24h^{-1} was observed with ceric ammonium nitrate (CAN) at pH 0.7 and with NaIO_4 at pH 4.7, respectively. A new peak at 749 nm for the catalyst **49** and at 731 nm for the catalyst **50** in the UV-Vis spectrum was detected after the addition of small amount of CAN to the solutions of **49** and **50**. Catalysts **51-55** did not exhibit such type of behaviour. These absorbance bands were in agreement with the formation of $[\text{Fe}(\text{IV})(\text{N}_4)\text{O}]^{2+}$ during water oxidation reaction. However, the speedy deactivation was observed for the complex **49** because of the ligand oxidation during the catalytic cycle.

5. Fe Complexes as Precatalyst for Water Oxidation:

The conversion or degradation of homogeneous Fe catalysts into nanoparticles due to the oxidation of ligand throughout the oxidation process is a crucial issue for the researchers. This issue of homogeneous *versus* heterogeneous water oxidation driven by iron complexes actually ought to be justified from the viewpoints of the practical applications of Fe-complexes as catalysts for water oxidation reaction.

The catalytic activity of bi-, tri-, and tetra dentate N-based Fe-complexes as catalysts for the oxidation of water to dioxygen were examined using both of the chemical and photochemical methods at pH 7-9.⁹⁹ The catalyst *cis*- $\text{Fe}(\text{mcp})\text{Cl}_2$ **58** (mcp is $\text{N,N}'\text{-dimethyl-N,N}'\text{-bis(2-pyridylmethyl)cyclohexane-1,2-}$

diamine with $(\text{NH}_4)_2\text{Ce}(\text{NO}_3)_6$ as the oxidizer in unbuffered water afforded plenty of turnovers, a TON of 290 ± 15 was reached. However, replacement of CAN with $[\text{Ru}(\text{bpy})_3](\text{ClO}_4)_3$ as the oxidizer in the solution of borate buffer (pH 7-9), no O_2 was detected from the same complex. Complexes $[\text{Fe}(\text{bpy})_2\text{Cl}_2]\text{Cl}$ **56**, $[\text{Fe}(\text{tpy})_2]\text{Cl}_2$ **57**, *cis*- $[\text{Fe}(\text{cyclen})\text{Cl}_2]\text{Cl}$ **59**, and *trans*- $\text{Fe}(\text{tmc})\text{Br}_2$ **60** (tpy is 2,2':6',2''-terpyridine, cyclen is 1,4,7,10-tetraazacyclodecane, and tmc is 1,4,8,11-tetramethyl-1,4,8,11-tetraazacyclotetradecane) were applied as catalysts. The O_2 evolution promptly happened with turnover numbers (TON's) starting from 19 to 108. Catalysts **56-60** were also examined for photochemical water oxidation using $[\text{Ru}(\text{bpy})_3]\text{Cl}_2$ as photosensitizer and $\text{Na}_2\text{S}_2\text{O}_8$ as oxidant in borate buffer (pH 7.5-9). Notably $\text{Fe}(\text{mcp})\text{Cl}_2$ **58**, which was not active in the chemical oxidation, showed a good activity under photochemical conditions. DLS measurements proved that nanoparticles were produced during light-driven water oxidation with all the screened Fe-complexes. The particles were isolated and determined to be Fe_2O_3 utilizing numerous analytical methods such as XPS (X-ray photoelectron spectroscopy) and energy-dispersive X-ray spectroscopy. ESI/MS studies of the catalysts in aqueous solutions at pH 7-9 demonstrated the formation of considerable amounts of free cyclen, tmc, and bpy substance from the solution of $[\text{Fe}(\text{cyclen})\text{Cl}_2]\text{Cl}$ **59**, $\text{Fe}(\text{tmc})\text{Br}_2$ **60**, and $[\text{Fe}(\text{bpy})_2\text{Cl}_2]\text{Cl}$ **56** in 1 minute. This steered that the discovered chemical activity of those complexes arose from $\text{Fe}^{3+}(\text{aq})$ ions generated before oxidation.

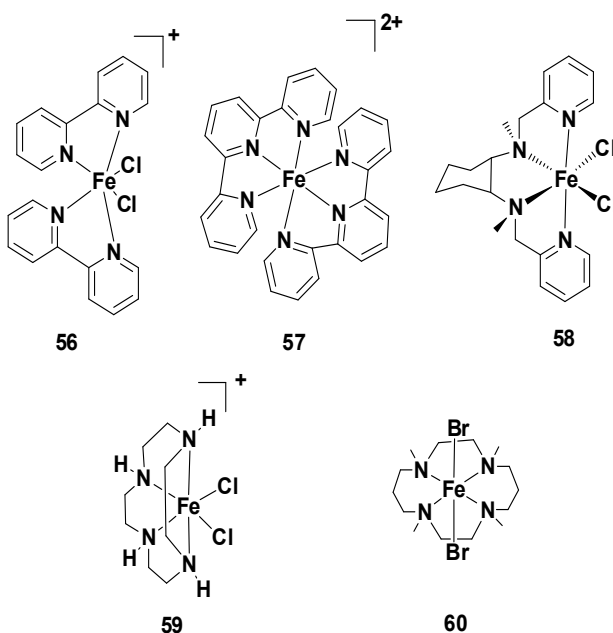


Figure 17 Structures of iron complexes performed as heterogeneous WOCs.

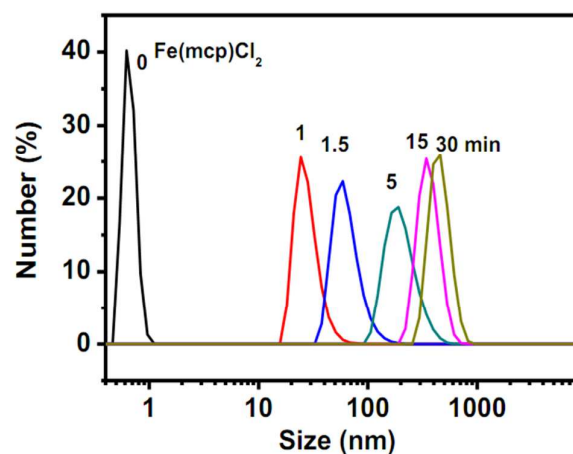


Figure 18 Particle size distribution examined by DLS measurements. Particles produced by irradiation (Xe lamp, 200W, $\lambda > 420$ nm) of a solution of $10 \mu\text{M}$ **58** containing 0.2mM $[\text{Ru}(\text{bpy})_3]\text{Cl}_2$ and 2mM $\text{S}_2\text{O}_8^{2-}$ in 15mM borate buffer (pH 8.5)

The photochemical oxidation of water was performed using catalyst **47** (Figure 14) in the solutions of a borate buffer at pH 8.0, 8.5 or 9.0 containing 5.0mM $\text{Na}_2\text{S}_2\text{O}_8$, and 0.25mM $[\text{Ru}(\text{bpy})_3]\text{SO}_4$. The evolution of O_2 was not ascertained in the absence of the catalyst **47** under the same reaction conditions. The quantity of O_2 formation after 20 min illumination at pH 9.0 ($2.6 \mu\text{mol}$, $\text{TON}'\text{s}=259$) was larger than those at pH 8.5 ($2.4 \mu\text{mol}$, $\text{TON}'\text{s}=238$) and 8.0 ($0.67 \mu\text{mol}$, $\text{TON}'\text{s}=67$). A maximum O_2 yield was 52% at pH 9.0. Nanoparticles from the catalyst **47** were observed by DLS measurements (Figure 19) and these nanoparticles acted as a real catalyst during the photochemical water oxidation reaction. Nanoparticles were also produced throughout the oxidation reaction by the catalyst **48** at pH 9.0. No O_2 formation was detected when 50mM phosphate buffer (pH 8.0) were used for photochemical water oxidation. Dissolved Fe^{2+} ions were precipitated as $\text{Fe}_3(\text{PO}_4)_2$ in the phosphate buffer solution. The nanoparticles produced during the photochemical oxidation of water by $\text{S}_2\text{O}_8^{2-}$ with **47** at the initial pH of 9.0 were analysed by XPS and TEM measurements and these studies concluded that the particles were $\text{Fe}(\text{OH})_x$.

The decomposition of iron catalysts during water oxidation due to the ligand oxidation is the critical issue and these issues on homogeneous vs. heterogeneous water oxidation should be clarified especially from the significance of the potential application of iron complexes as catalyst for water oxidation. The water oxidation activity of iron complex catalysts is extremely susceptible to electronic and structural factors. The incorporation of intramolecular H-bonding functionalities within the structure of molecular iron catalysts can provide future directions for designing new promising WOCs. As well as the choice of ligand platforms able to support the reactive metal-oxo substances essential for catalysis, the selection of operating conditions might afford iron catalysts with high TOFs and lower overpotential

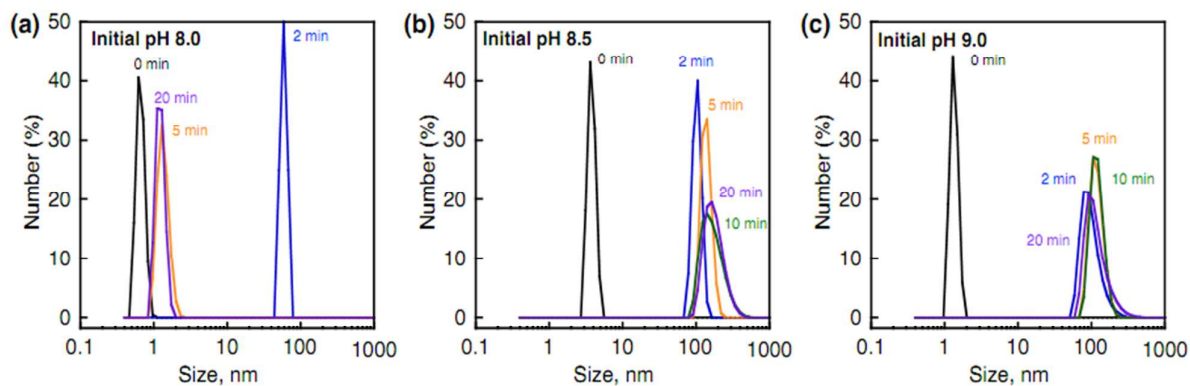


Figure 19 Particle size distribution examined by DLS measurements of a solution containing $50 \mu\text{M}$ **47**, 5mM $\text{S}_2\text{O}_8^{2-}$ and 0.25mM $[\text{Ru}(\text{bpy})_3]\text{SO}_4$ in borate buffer at different pH at illumination times of 2.0 min (blue line), 5.0 min (orange line), 10 min (green line), and 20 min (purple line). The black solid line for particle size in the absence of **47** at 0 min.

6. Ni (II) Complexes as Homogeneous Water Oxidation Catalysts:

Science plays a vital role in the planning and research on the latest catalysts supported abundant metals at its heart. The development of homogenous WOCs supported nickel has been comparatively unknown. To the best of our knowledge, there is just one molecular nickel complex that can act as homogeneous WOCs.

Zhao *et al.* claimed the first Ni-based homogeneous WOCs, $[\text{Ni}(\text{meso-L})](\text{ClO}_4)_2$ (L is 5,5,7,12,12,14-hexa-methyl-1,4,8,11-tetraazacyclotetradecane **61** which electro-catalysed the oxidation reaction of water at low overpotential and neutral pH in phosphate buffer.¹⁰⁰

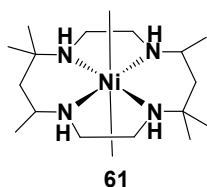


Figure 20 The Structure of $[\text{Ni}(\text{meso-L})]^{2+}$ works as homogenous catalyst for WO.

$73 \mu\text{mol}$ of O_2 were observed after 6 h of electrolysis at 1.55V vs. NHE (ca. 730mV overpotential), with a turnover number (TON's) of 15 and a Faradaic efficiency of 97.5%. The ESI-MS, CV, and UV-Vis spectra of the ensuing resolution after 6h electrolysis were examined and it was observed that the ESI-MS, CV, and UV-Vis spectra of the ensuing solution were nearly similar to those of the solutions prior to electrolysis, suggesting the catalyst **61** did not decompose throughout the electrolysis reaction. Furthermore, the solution of the catalyst after 6 h of continuous electrolysis was evaporated very slowly obtaining crystals of $[\text{Ni}(\text{meso-L})](\text{ClO}_4)_2$ and single crystal X-ray analysis of the obtained crystals indicated that the molecular structure of the catalyst **61** remains unchanged, indicating that catalyst **61** is a

strong and long-lasting WOC. To examine if the water oxidation reaction by $[\text{Ni}(\text{meso-L})](\text{ClO}_4)_2$ was homogeneous or heterogeneous, the authors also performed successive scanning of 1mM $[\text{Ni}(\text{meso-L})](\text{ClO}_4)_2$. The catalytic current decreases with consecutive scanning and becomes virtually constant when reaching 10 scan cycles. On the other hand, CV of other Ni-based heterogeneous catalysts showed a rise in catalytic current with continual scanning that was ascribed to the deposition of NiOx as WOCs from the catalytic system. It was confirmed from different CV behavior that $[\text{Ni}(\text{meso-L})](\text{ClO}_4)_2$ was a truly homogeneous WOC. Controlled potential electrolysis on ITO electrode for 6h at $+1\text{V}$ did not led to deposition of any film on the ITO electrode as confirmed from SEM measurements. EDS (Energy-dispersive X-ray spectroscopy) study conjointly confirmed that no elemental P or Ni was existed on the ITO electrode. A further line of evidence was gained from DLS measurements which confirmed that no nanoparticles were produced in the solution of the catalyst **61** after electrocatalysis. The chemical process current density of the catalytic system increased linearly with the concentration of the Ni-complex **61**, indicating a single-site metal catalysis. Furthermore, instant precipitation occurred by the addition of 1mM $\text{Ni}(\text{NO}_3)_2$ solution to the 0.1M phosphate buffer solution. Moreover, this mixture did not show any catalytic activity for the oxidation of water, indicating that the water oxidation was attributed to the molecular Ni-catalyst rather than free Ni^{II} ions in the solution. Therefore, electrocatalytic water oxidation by $[\text{Ni}(\text{meso-L})](\text{ClO}_4)_2$ was homogeneous on either ITO or GC electrode.

7. Ni (II) complexes as heterogeneous WOCs:

Although Nickel is an earth-abundant metal, still its activity for water oxidation is unexplored. To the best of our knowledge, there are only a few reports within the literature concerning molecular nickel complexes that can act as a precatalyst for the water oxidation reaction.

Tai-Chu Lau and co-worker reported a series of Ni^{II} complexes **62-67** bearing multidentate N-donor ligands that serve as a precatalyst and converted into Ni-oxide nanoparticles under experimental conditions. These nanoparticles acted as true for

water oxidation reaction.¹⁰¹ Water oxidation activity of all the complexes was examined for chemical water oxidation reaction at pH 7.0-8.5 using $[\text{Ru}(\text{bpy})_3](\text{ClO}_4)_3$ as oxidant. Complex **62**, which incorporates a hexadentate ligand, produced very little quantity of O_2 upon addition of the oxidant, $[\text{Ru}(\text{bpy})_3]^{3+}$. On the other hand, complexes **63-67** yielded more amount of O_2 in borate buffer at pH 8.0 with turnover numbers (TONs) and turnover frequencies (TOFs) that ranged from 31-54 and 0.19-0.42s⁻¹, respectively. The yield of O_2 for the chemical water oxidation reaction by **67** was negligible at pH <7.5; however the turnover

frequency increased with increasing pH from 7.5 to 8.5. Moreover, the TON first increased with a pH-increase from 7.5 to 8.0 thereafter a drop in the TON was observed with a further increase of the pH to 8.5, which could be attributed to the rapid decomposition of $[\text{Ru}(\text{bpy})_3]^{3+}$ at high pH. Upon increasing the concentrations of the oxidant $[\text{Ru}(\text{bpy})_3]^{3+}$ from 0.25-1.5mM, the O_2 yield was also improved indicating the deactivation of the catalysts. The photochemical water oxidation by the catalysts **62-67** in borate buffer at pH 7.0-8.5 was also checked using $[\text{Ru}(\text{bpy})_3](\text{ClO}_4)_2$ as PS and $\text{Na}_2\text{S}_2\text{O}_8$ as the oxidizer.

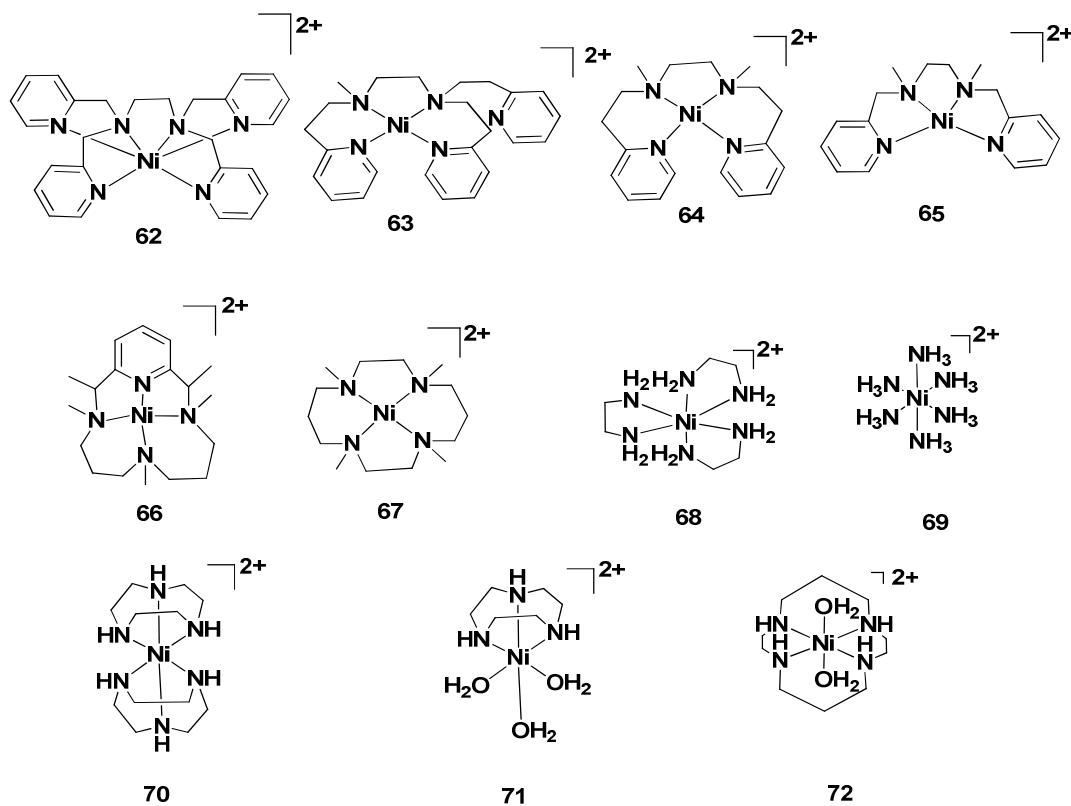


Figure 21 Structure of nickel (II) complexes used as precatalysts.

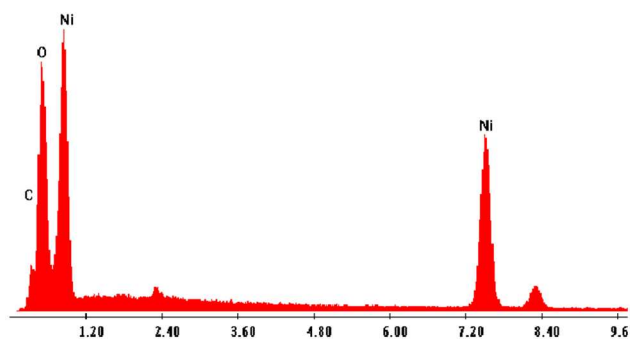


Figure 22 EDX spectrum of particles produced after photochemical water oxidation.

While complex **62** was completely inactive towards photochemical water oxidation, complexes **63** and **65** showed maximum TON's up to 813 and 855 respectively. To know about the real catalyst for the water oxidation catalysis, DLS measurements were used to investigate the presence of any nanoparticles produced during the photochemical water oxidation. Indeed particles were generated during photocatalytic water oxidation from all screened Ni-complexes except **62** that showed no activity. The SEM image displayed that the nanoparticles formed during the catalytic process were composed of submicron particles and from EDX (Energy-dispersive X-ray) spectroscopy (Figure 22) the presence of Ni and O was confirmed. Similarly, Spiccia and his research group disclosed a series of molecular nickel catalysts that decomposed into heterogeneous NiOx during catalytic oxidation process.^{102, 103} Different types of complexes such as Ni(en)₃²⁺ **68**, Ni(NH₃)₆²⁺ **69**, Ni(tacn)₂²⁺ **70**, Ni(tacn)(OH₂)₃²⁺ **71**, and Ni(cyclen)(OH₂)₂²⁺ **72**, were oxidized to produce NiOx films on ITO electrodes in borate buffer at pH 9.2 when the potential was scanned up to 1.3V vs. Ag/AgCl. The analysis of the films by various techniques such as EDX, Raman, EXAFS/XANES and SEM indicated that the NiOx substances were similar to other NiOOH catalytic substances. Surprisingly, no detectable NiOx materials were produced from any of the catalysts except for the control with Ni(H₂O)₆²⁺ when the potential was scanned up to 0.85V vs. NHE. This result suggested that the steadiness of a catalyst before catalytic oxidation cannot guarantee about the steadiness of the catalyst for more oxidizing reaction conditions. The enhancement in catalytic activity with the increasing of electroactive surface area of nickel oxide films was another result from the same studies. Though the catalytic activity depending on surface area is the most documented in the field of heterogeneous catalysis, this finding reinforces the necessity to think about and account for the effect of catalyst's surface area and numbers of active sites in control experiments geared toward ruling out the presence of heterogeneous water oxidation catalysts.

It is apparent that more work should be done in the area of water oxidation catalysis with molecular nickel complexes to extend the robustness and activity of catalysts. Stability of these catalysts is the key concern. Consequently, scientist should give special attention to the issue of stability of molecular nickel complexes when used as catalyst for water oxidation reaction.

8. Cu Complexes Acting as Homogeneous WOCs:

Molecular copper complexes as water oxidation catalysts have seldom been studied. This is probably to the metal's priority to bear one-electron instead of a two-electron redox process. To the best of our knowledge, only four families of copper-based homogeneous WOCs are reported.

Mayer and co-workers first reported a copper-based homogeneous water oxidation electrocatalyst.¹⁰⁴ The notable characteristics of the catalyst **73** (Figure 23) is the self-assembling at the proper basic pH from bipyridine and normal Cu-salts. Electrochemical measurements confirmed that the complex [(bpy)Cu(OH)₂] was the resting state. The turnover frequency of this catalytic system was 100s⁻¹. Cyclic voltammograms were measured of three water soluble [(bpy)Cu(μ-OH)]₂X₂ salts (where X₂=(OAc)₂, (OSO₂CF₃)₂[(OTf)₂]) and SO₄²⁻ at pH 11.8–13.3. All the three copper salts showed pH dependant irreversible and large oxidation waves at +1.3–1.5 V, which was indicative for catalysis. Catalysis occurred at about 750 mV overpotential and gas bubbles were formed on the electrode surface over several scans. An intense irreversible peak was seen at -0.3V when the electrode was cycled to cathodic directions after scanning through anodic directions indicating that the oxidative catalysis formed O₂. To identify the responsible materials for the electrocatalytic oxidation process, EPR (electron paramagnetic resonance) analyses of the solutions after electrolysis were studied. EPR spectra showed a simple quartet and confirmed that the monomeric complex [(bpy)Cu(OH)₂] was the catalyst for water oxidation reaction. Several evidences suggested that this catalytic system was homogeneous. The electrodes were totally free from discoloration throughout the bulk electrolysis and cyclic voltammetry experiment.

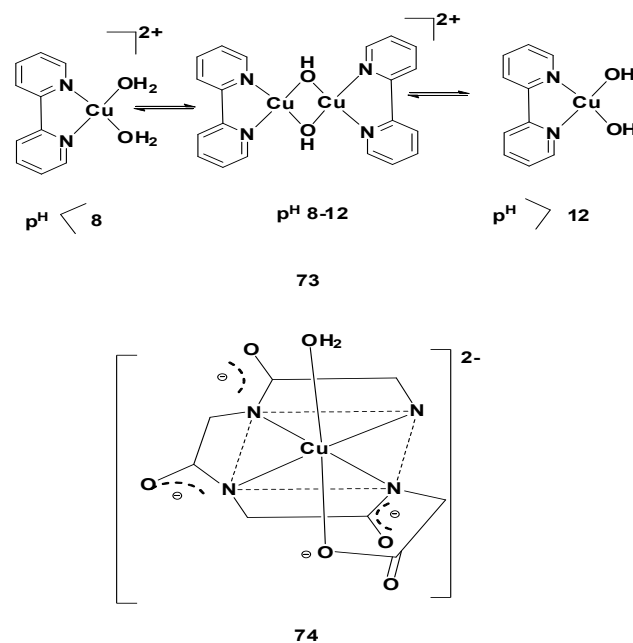


Figure 23 Copper catalysts for homogeneous water oxidation

The obtained maximum current in the CVs did not increase over multiple scans and the shape of the wave did not change also. No new peaks were seen in the optical spectra of the solutions after electrolysis. For further confirmation, the working electrode (GC electrode) was cycled ten times in the solutions of [(bpy)Cu(μ -OH)]₂(OAc)₂ with 0.1M acetate buffer (pH 12.5). Then the working electrode was washed only with water but not polished. The electrode was scanned further in only fresh buffer solution of the same pH. No catalytic current was produced in this case and it was concluded that the Cu system was a homogeneous electrocatalyst.

Cu^{II}-complex of the macrocyclic ligand (triglycylglycine, TGG⁴⁻) **74** efficiently catalysed oxidation of water to dioxygen in phosphate buffer (pH 11).¹⁰⁵ ATOF of 33s⁻¹ was achieved with this system. In the CV, a reversible oxidation wave appeared at E_{1/2}=+0.58V vs. NHE with a peak-to-peak separation of ΔE_p =70mV at a10mV/s scan rate. This was according to a reversible oxidation of Cu(II) of [(TGG⁴⁻)Cu^{II}-OH₂]²⁻ to Cu(III) by a PCET process to produce the hydroxyl compound, [(TGG⁴⁻)Cu^{III}-OH]²⁻. Another irreversible oxidation appeared at E_{p,a}=1.32V vs. NHE in 0.25M phosphate buffer (pH 11) at more positive potentials. The reversible oxidation wave for the [(TGG⁴⁻)Cu^{III}-OH]²⁻/[(TGG⁴⁻)Cu^{II}-OH₂]²⁻ couple was seen on reverse scanning in the CV without loss of peak current which is according the catalytic water oxidation process instead of oxidative decomposition of the catalyst. This current increment for the wave at E_{p,a}=1.32V was conjointly according to water oxidation catalysis. The onset for the oxidation of water appeared at ca. 1.10V vs. NHE with an overpotential of ca.0.52V. The complex, not free Cu (II), was responsible for water oxidation. Cu₃(PO₄) and/or Cu(OH)₂ solution /suspension formed from the 1 mM CuSO₄ in the solution of phosphate buffer (0.25M, pH 11) had no activity toward water oxidation. O₂ evolution was examined by 2mM [(TGG⁴⁻)Cu^{II}-OH₂]²⁻ in phosphate buffer (0.25M, pH 11) on an ITO electrode with a large surface area (0.70cm²) by controlled potential electrolysis at +1.3V. The catalytic current was set for a minimum of 5h at a constant current density of 0.80mA/cm². The current slightly decreased with diminishing of the pH by 1.5 units after 5 h electrolysis, which was in agreement with the consumption of hydroxide ions (OH⁻) in the water oxidation reaction. The original current density was recovered again after adjusting the pH of the solution to the initial or original value (pH 11) and the current density was sustained for a supplementary 5h. There was no proof found for nanoparticles or film formation by XPS, SEM after 2h electrocatalysis under similar conditions. These studies confirmed that the complex was a true homogeneous catalyst.

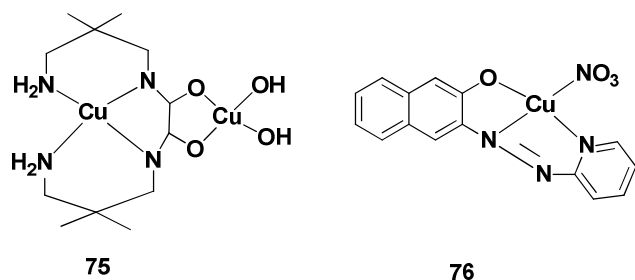


Figure 24 Copper complexes acting as homogeneous WOCs.

Complex **75**, [Cu(Me₂oxpn)Cu(OH)₂] (Me₂oxpn= N,N'-bis(2,2'-dimethyl-3-aminopropyl)oxamido) is the first soluble electrocatalyst for water oxidation and reduction reaction.¹⁰⁶ Water oxidation catalysis happened at the overpotential of 636 mV vs. SHE and a turnover frequency of ~2.14s⁻¹ was achieved using this system at pH 10.4. Cyclic voltammetry studies of the complex **75** were performed in a buffer solution with different pH and two irreversible oxidation peaks similar to Cu^{III}Cu^{II}/Cu^{II}Cu^{II} and Cu^{III}Cu^{III}/Cu^{III}Cu^{II} were observed at 0.90 and 1.26V vs. Ag/AgCl in the 0.25M buffer solution. The CV of the solution without catalyst showed no catalytic current and this result confirmed that water oxidation catalysis occurred with catalyst **75**. A bulk electrolysis experiment of the aqueous solution of catalyst **75** (5.74mM) in 0.25M phosphate buffer using an ITO electrode at different potentials showed that the quantity of charge utilized in a pair of minutes increased with rising potential, related to the formation of a huge quantity of gas bubbles which was caused by the formation of O₂ from H₂O. O₂ evolution from this catalytic system was examined by CPE measurement at 1.23V vs. Ag/AgCl on an ITO electrode with a large surface area (1.32cm²) in phosphate buffer (0.25M and pH 10.4) with 2.8mM catalyst **75**. The pH of the solution after 5 h electrolysis reaction was reduced by 2.0 units, in line with the consumption of OH⁻ ion by the oxidation of water, 4OH⁻ + 4e⁻ ↔ 2O₂ + 2H₂O. The produced O₂ amounted to ~38.8 mmol (quantified by GC) with a 90% Faradaic efficiency. The stability of complex **75** as electrocatalyst was studied in an extended control potential electrolysis (CPE) measurement carried out in 0.25M buffer solution at pH 7.0 and pH 10.4 respectively. No significant loss in catalytic activity was noted during the water oxidation catalysis for 72 h, suggesting that complex **75** was a robust catalyst. The catalytic current was dependent on the concentration of the complex, indicated that it was a homogeneous catalyst. Moreover, the electrode was washed with distilled water and electrolysis of the solution without catalyst was made for 2 min at -1.45V vs. Ag/AgCl in phosphate buffer (0.25M and pH 7.0). Throughout this reaction time, ca. 128mC of charge was passed, the same magnitude as was established for the electrolysis reaction carried out with freshly polished electrodes. There was no change in colour of the electrode surface during cyclic voltammetry and bulk electrolysis experiments. An ICP study also confirmed that no precipitate was formed on the surface of GC electrode after 2 h electrolysis under the same reaction conditions.

Complex **76** acted as robust catalyst for chemical water oxidation and showed an initial TOF of 4.0kPa h⁻¹.¹⁰⁷ The CVs of the catalyst **76** were performed in water, phosphate buffered saline (PBS) was used as supporting electrolyte at ambient temperature with the scan rate of 50mV/s. The cyclic voltammetry studies of the complex were carried out within the pH range of 8.0-13.0 and the concentration range of 0.1mM - 1.0 mM. The cyclic voltammogram exhibited large irreversible oxidation peaks, which were due to water oxidation catalysis. The i_p peaks were observed at 0.995V when the concentration of the complex **76** was ≤ 0.6mM and it was ascribed to the oxidation reaction of Cu(II) → Cu(III). A complicated behaviour was seen at pH 11, during which a peak in the CV was additional abrupt with rising concentration which was assigned to polymerization or oligomerization of the catalyst **76**. At pH 11, the i_p

peaks amplified with the rising of the complex concentration **76** and became almost linear, which is in line with single-site Cu catalysis. No oxidation peaks were observed at the potential range from 0 to 1.5V at pH <11. A single i_p peak was seen in the CVs at the potential range from 0.8 to 1.0V when the pH value was >11. On the other hand, double i_p peaks occurred at 1.0V for pH=11. So, the oxidation behaviour of the catalyst **76** was clearly pH dependent. Examination of the O₂ released applying different solvents was performed. Dissolving the Cu catalyst in CH₃OH, the catalytic activity was higher than in CH₃CN confirming that the released oxygen was not deriving from CH₃OH but from H₂O.

9. Cu Complexes Acting as Heterogeneous WOCs:

Cu^{II}-complexes are excellent targets for water oxidation catalysis due to their biomimetic chemistry with O₂. There is only a single report of a molecular copper complex which acts as WOCs in heterogeneous conditions.

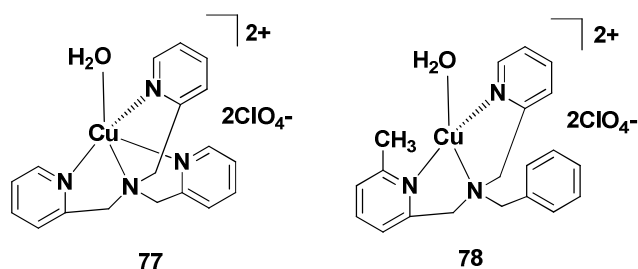


Figure 25 Copper (II) complexes used as precatalyst for water oxidation.

Du and co-workers reported a heterogeneous catalytic system for water oxidation reaction that was constructed of a supported nanostructured Cu-oxide electrodeposited from molecular Cu(II)-2-pyridylmethylamine complexes **77-78** (Figure 25).¹⁰⁸ The cyclic voltammograms (CVs) of complex **77** using a FTO electrode showed an oxidation wave at about 1.2 V at pH 9.2. O₂ bubbles were confirmed by gas chromatography and fluorescence based O₂ sensor suggesting that water oxidation catalysis happened throughout the anodic scan. The current density for this catalytic system was extremely pH dependant. The maximum current intensities were measured when the pH was brought to 11.0. The CVs, employing a glassy carbon electrode, presented an oxidative catalytic current peak at $E_{p,a} \sim 1.65V$ and a current crossover appeared in the reverse scan. These observations indicated that high oxidation state copper intermediates were produced during oxidation reaction. The catalytic current densities increased with increasing pH and O₂ gas were produced on the FTO electrode during the bulk electrolysis of the complex **77** at 1.41V. A grey metal film was observed on the surface of FTO electrode within one hour from pH 9.2 to 11.0 that became darker with the extension of the electrocatalysis time. In addition, the film deposited on the electrode was used for the bulk electrolysis experiment in a borate buffer solution containing no Cu(II)-complex where a similar current intensity and O₂ gas bubbles were detected confirming the high catalytic activity of this film. CV measurements revealed that complex **78** is also an active precatalyst for

electrocatalytic water oxidation. SEM images of the deposited films on the electrode at 1.41V clearly displayed that nanostructured species were produced throughout the water oxidation catalysis. Moreover, XPS analysis of the electrodeposited films at pH 9.2 and 11.0 revealed that the films were mainly composed of Cu and O, these CuO films were found to be amorphous from XRD spectra. Finally, it was confirmed from the Faradaic efficiency (> 90%) that the catalysts were able to convert water into dioxygen under a moderate overpotential.

Cu-based molecular WOCs discussed above have shown high current densities and good stabilities even under basic conditions. Nonetheless, the main problem with these systems is their high overpotentials for the water oxidation reaction due to copper intermediates (Cu^{III} and/or Cu^{IV}) with high oxidation-state. Therefore, it is highly desirable to find out new strategies to lower overpotentials of these copper-based water oxidation catalysts.

10. Manganese complexes as catalysts for homogeneous water oxidation:

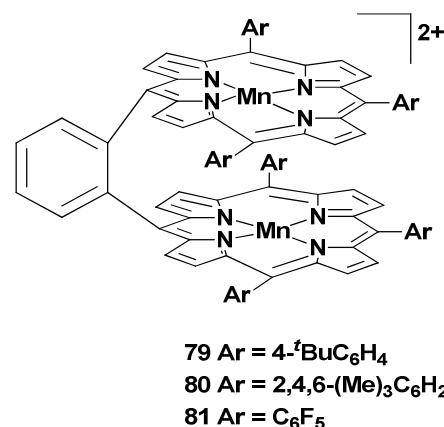


Figure 26 Manganese porphyrin complexes for water oxidation

Naruta and co-workers used binuclear manganese complexes **79-81** as catalysts for water oxidation.¹⁰⁹ All three manganese complexes showed a similar irreversible rise in current at ≥ 1.4 V (vs NHE) in aqueous acetonitrile solutions (5% v/v H₂O in CH₃CN) containing *n*Bu₄NOH. Moreover, no O₂ was evolved from anodic oxidation of the aqueous acetonitrile solution without the complexes **79-81** in the potential range up to + 2.5 V (vs. NHE). All three complexes exhibited O₂ evolution at a potential range from +1.2 to +2.0 V. Out of these complexes **79-81**, complex **81** was the best performing catalyst for the water oxidation reaction with a maximum TON of 9.2. The rate of O₂ evolution was proportional to the concentration of the used manganese catalyst **79-81**, confirming its involvement in the rate-determining step. ¹⁸O-Labeling experiments confirmed that both oxygen atoms in the evolved O₂ originated from the solvent H₂O.

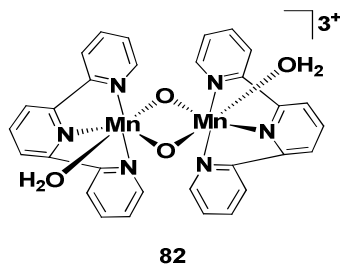


Figure 27 Structure of $[(\text{H}_2\text{O})(\text{tpy})\text{Mn}(\mu\text{-O})_2\text{Mn}(\text{tpy})(\text{OH}_2)]^{3+}$ complex.

In 1999, Crabtree and Brudvig research group introduced the first manganese catalyst, $[(\text{H}_2\text{O})(\text{tpy})\text{Mn}(\mu\text{-O})_2\text{Mn}(\text{tpy})(\text{OH}_2)]^{3+}$ ($\text{tpy} = 2,2':6',2''\text{-terpyridine}$) **82** for chemical water oxidation.¹¹⁰⁻¹¹² Afterwards, a series of substituted derivatives of this complex has been prepared and examined for their water oxidation ability.^{113, 114} Crystal structure of **82** showed that it was a mixed valence dimer containing two exchangeable H_2O molecules, one on each Mn center. This two exchangeable aqua ligands played a fundamental role for the reactivity of complex **82** for water oxidation when sodium hypochlorite (NaOCl) was used as chemical oxidant.¹¹⁰ 12.5 μM solution of catalyst **82** in 0.07M aqueous NaOCl (pH 8.6) produced O_2 with an initial rate of 12 ± 2 mole hour^{-1} per mole of **82** and four catalytic turnovers over 6 hours. The water oxidation reaction ended with the complete conversion of Mn into inactive permanganate. The formation of inactive permanganate during the catalytic reaction could be examined by UV-Vis spectroscopy. UV-Vis and EPR analyses suggested that the complex primarily reacted vigorously to produce a IV/IV dimer without EPR signal which was the major species in the catalytic process. $\text{Mn}(\text{V})=\text{O}$ intermediates were formed during the reaction between the IV/IV dimer and NaOCl that was responsible for O-O bond formation step.¹¹⁸ ^{18}O -Labeling experiments confirmed that 75% of the evolved O_2 originated from the solvent H_2O and the rest of the evolved O_2 derived from the oxidant ClO^- . The authors proposed a mechanism of water oxidation reaction using catalyst **82** on the basis of isotopic distribution and it was clear from the mechanistic studies that this catalyst was homogeneous in nature. Later on, more studies revealed that catalyst **82** could catalyse water oxidation more efficiently when oxone (KHSO_5) was used as chemical oxidant instead of NaOCl .^{111, 115-117} The catalytic performance of this system was highly dependent on the ratio of **82** and oxone. The major amount of complex **82** was converted into inactive permanganate when 1: 500 ratio was used and $< 10\%$ of oxygen content in the evolved oxygen derived from the solvent H_2O . However, when 1: 100 ratio was used, 50% of the evolved O_2 originated from H_2O . A major disadvantage of catalyst **82** was the requirement of using oxidants to facilitate the water oxidation. Although successive study by the same research group disclosed that it was possible to perform water oxidation using **82** together with a Ce^{IV} oxidant.¹¹⁸ Many other studies also dismissed the issue of the limitation of using oxidants with the catalyst **82**.¹¹⁹⁻¹²¹ A tetranuclear manganese complex, a so-called “dimer of dimers” complex can be formed by the oxidation of **82**.^{122, 123} Deronzier’s research group disclosed that this tetranuclear manganese complex was not able to perform water oxidation

electrochemically¹²⁰, while a more recent work of Brudvig and Crabtree published contradictory findings where they claimed that “dimer of dimers” complex was able to drive electrochemical oxidation of H_2O to O_2 with a turnover number of 2.8.¹²⁴ Finally, it can be concluded that water oxidation by catalyst **82** is intricate and mainly depends on the reaction conditions.

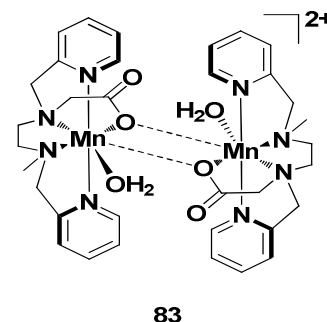


Figure 28 Molecular structure of the complex, $[\text{Mn}_2^{\text{II}}(\text{mcbpen})_2(\text{H}_2\text{O})_2]^{2+}$.

Complex $[\text{Mn}_2^{\text{II}}(\text{mcbpen})_2(\text{H}_2\text{O})_2]^{2+}$, **83** (Where mcbpen = *N*-methyl-*N'*-carboxymethyl-*N,N'*-bis(2-pyridylmethyl)ethane-1,2-diamine) acts as an active catalyst for water oxidation reaction.^{125, 126} Treatment of complex **83** with *tert*-butyl hydroperoxide (TBHP) in H_2O resulted in a change of the initial color of the solution from pale to brown due to the oxidative cleavage of the dimeric structure of **83** into two monomeric $\text{Mn}^{\text{III}}\text{-OH}$ or $\text{Mn}^{\text{III}}\text{-OR}$ species. Moreover during this treatment gas bubbles were observed. It was confirmed using membrane inlet mass spectrometry (MIMS) and a Clark electrode that the gas formation from the reaction between **83** and TBHP in H_2O was really O_2 . ^{18}O -labelling measurements confirmed that one oxygen atom in the evolved O_2 originated from H_2O while the other one from the oxidant TBHP. Later, more detailed catalytic experiments were conducted in which 20 equivalents of TBHP were added stepwise (four times) to a 0.5 mM solution of **83**. This system produced 1.06 mmol of O_2 , which was tantamount to a turnover number of 6.2. Control experiments using $\text{Mn}(\text{ClO}_4)_2$ as catalyst instead of **83** under the same conditions proved the absence of O_2 generation, confirming the unique activity of **83**. Complex **83** was also investigated as catalyst for water oxidation using a nonoxygen transfer oxidant, CAN. When Ce^{IV} was considered as oxidant to perform water oxidation, just one oxygen atom in the evolved O_2 derived from the solvent H_2O and the other one was probably from the nitrate ion of the oxidant but no concrete evidence of the nitrate ion reduction was provided. It was concluded from different spectrometric methods (UV-Vis, EPR and MS) that several types of high valent manganese species, not nanoparticles, were responsible for the water oxidation reaction.

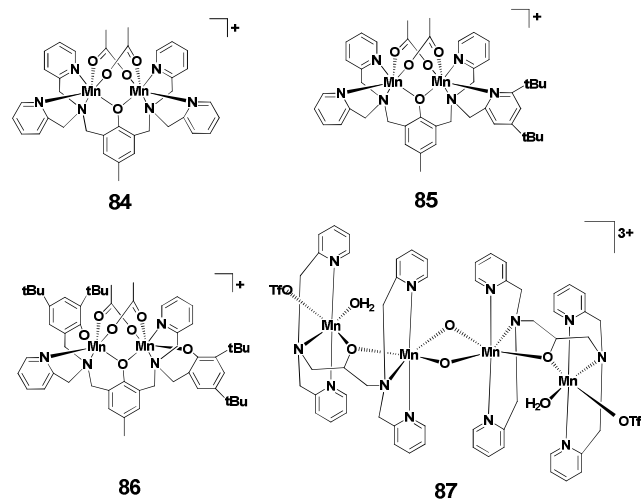


Figure 29 Manganese complexes working as WOCs.

Anderlund *et al.* prepared tetranuclear Mn-complex **87** and some other related tetranuclear manganese complexes^{119, 127, 128}, which showed a high resemblance with complex **83** (Figure 29). The ultimate aim was to perform an evaluation of the water oxidation activity of complexes **82**, **83**, and **84–87** under identical reaction conditions, utilizing different types of oxidants. Deoxygenated aqueous solutions of the complexes were taken into the reaction chamber of a Clark-type polarographic oxygen electrode after which an excess amount of different oxidants was added and O₂ evolution was measured. For this experiment, 2 mM solution of metal complex was used and 50 equiv of oxidant (except for H₂O₂ where only 2 equiv was added because of its disproportionation) was added to the metal solution.¹¹⁹ Based on the activity of the different oxidants; this systematic study established an activity trend for the manganese complexes for O₂ evolution reaction (H₂O₂ > Oxone > TBHP > ClO⁻). Moreover, mass spectrometry and EPR studies demonstrated that all these complexes (Figure 29) were homogeneous in nature under water oxidation conditions.

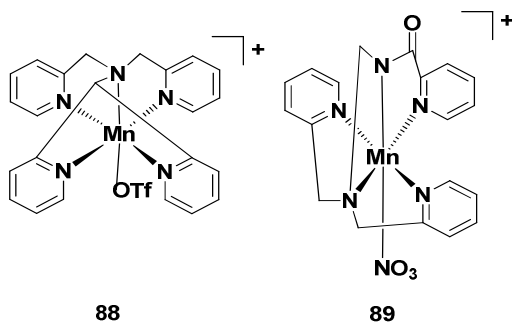


Figure 30 Molecular structures of manganese complexes **88** and **89** studied as WOCs.

Brudvig *et al.* studied the water oxidation activity of complexes **88** and **89** using oxone and H₂O₂ as oxidant.¹²⁹ Titration of **89** in aqueous Britton-Robinson buffer showed that this complex was stable between pH 2 and 10.5. Complex **88** was also stable in aqueous solution but it was hygroscopic and it showed O₂ evolution

only in the presence of H₂O₂ while **89** was active for O₂ evolution reaction in the presence of either oxone or H₂O₂. UV-Vis and EPR analyses were performed to learn about the responsible species for O₂ evolution. UV-Vis spectra of the complexes were taken in water before and after addition of 1 equiv. of oxone. Peaks at 375 and 465 nm in the spectrum of **89** were observed and were replaced within a few seconds after oxone addition having a higher molar absorptivity and a broad shoulder at 380 nm. The increase in molar absorptivity was attributed to the oxidation of Mn^{II} to Mn^{III} or Mn^{IV}. Complex **88** showed similar results. The UV-Vis spectra of the complexes were compared to the EPR results to identify the probable oxidation states of Mn during oxidation reaction. EPR spectra of the complexes fully supported the results of absorbance spectra. Complexes **88** and **89** were composed of pentadentate ligand frameworks and also contained pyridyl motifs as coordinating groups. The authors were able to show that the carboxamido group *trans* to the labile coordination site facilitated the formation of high-valent Mn substances which were able to mediate O₂ formation. It was due to the σ -donor capability of the carboxamido group that the Mn³⁺ resting state was stabilized and boosted the additional oxidation to higher oxidation states at lower potentials. This report revealed that ligand scaffolds with negatively charged groups can stabilize the Mn center(s) at high oxidation states and these characteristics are a valuable approach for designing Mn-based robust WOCs.

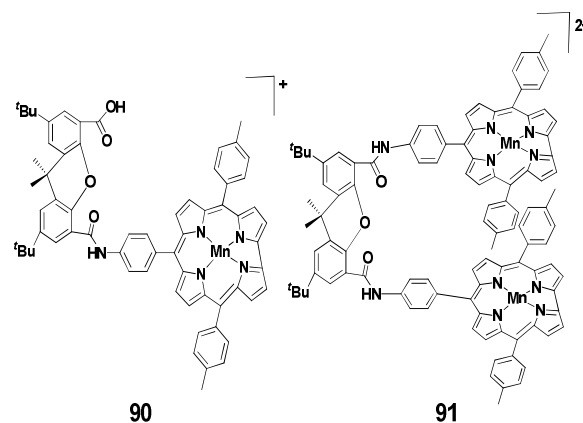


Figure 31 Manganese corrole complexes investigated for water oxidation.

A study published by Sun *et al.* reported that complexes **90** and **91** could catalyse water oxidation reaction at low potential (0.80V).¹³⁰ Electrochemical study of these two corrole complexes disclosed that Mn species with high-valent oxidation states could be formed at low potentials. Furthermore, there was an intramolecular interaction between two Mn centers in **91**, which could be very crucial in water oxidation catalysis. Water oxidation activity of complexes **90** and **91** was examined by cyclic voltammetric studies where scanning to anodic potential > 1.0V vs NHE exhibited a reduction peak at -1.09V due to the reduction of O₂. This feature also highly supported that these complexes could access high-valent oxidation states at low redox potentials.

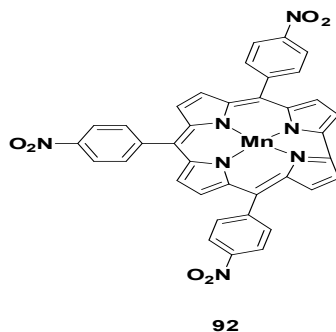


Figure 32 Mononuclear Mn^{III} corrole complex.

In 2009, the same research group prepared mononuclear Mn^{III} corrole complex **92** that was active for O₂ evolution reaction.¹³¹ Complex **92** produced Mn^V=O species after treatment with oxidant, TBHP and this Mn^V=O species generated O₂ after addition of *n*Bu₄NOH. The overall processes were examined by real-time MS and the catalytically active species during the processes were determined by a combination of HRMS and UV-Vis studies.

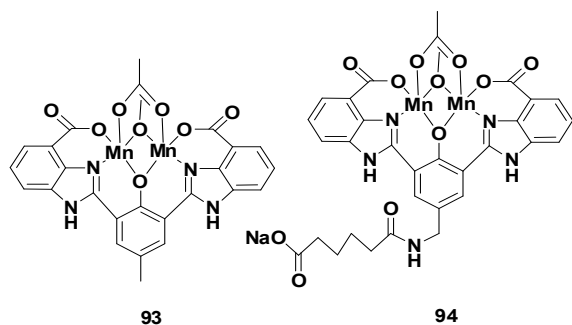


Figure 33 Dimeric manganese complexes studied as WOCs.

Complex **93** was the first example of WOCs which can homogeneously catalyse H₂O oxidation to molecular O₂ in the presence of single-electron oxidant, [Ru(bpy)₃]³⁺. Complex **93** was also able to catalyse photochemical water oxidation when [Ru(bpy)₃]²⁺ as photosensitizer and Na₂S₂O₈ as electron acceptor were used.¹³² Water oxidation activity of **93** was examined by addition of 480-fold excess of [Ru(bpy)₃]³⁺(PF₆)₃ in phosphate buffer (0.1M, pH 7.2). This system displayed immediately an O₂ evolution which lasted about 1 hour and gave a TON of ~25 and TOF of ~0.027s⁻¹. Control experiments using Mn(OAc)₂ or free ligand in replacement of **93** under same conditions confirmed that **93** was really responsible for O₂ evolution reaction. Light-driven water oxidation with **93** using [Ru(bpy)₃]²⁺ as PS and Na₂S₂O₈ as electron acceptor were conducted but this system gave only one turnover, which was due to the low oxidation potential of PS (1.26V vs NHE). Later, [Ru(bpy)₂(deeb)]²⁺ (deeb = 4,4'-bis(ethoxycarbonyl)-2,2'-bipyridine) was used as PS which has a higher oxidation potential (1.40V vs NHE) in replace of [Ru(bpy)₃]²⁺ proving that this system was more efficient producing a TON of 4. ¹⁸O-labelling experiments confirmed that both oxygen atoms in the evolved O₂ originated from the solvent H₂O. Behaviour of **93** in solution was examined in presence of K₃PO₄ by ¹H-NMR

spectroscopy and X-band EPR spectroscopy in D₂O and H₂O. No EPR signal at 77K was detected and the narrow chemical shift range confirmed the presence of a Mn₂^{III,III} complex which was the oxidized form of complex **93** (Mn₂^{II,III}). The cycle between Mn₂^{III,III} and Mn₂^{V,V} oxidation states of **93** was suggested during the course of water oxidation. In the EPR spectrum of **93** abroad (100mT) signal at *g* = 2.0 was observed from the reduction of Mn₂^{III,III} by ascorbic acid and no six-line signal of free Mn²⁺ was detected. These findings confirmed that **93** was intact under water oxidation conditions.

Inspired from the research work on **93**, Åkermark synthesized some similar dimeric Mn₂^{II,III} complexes containing different substituents in the *para* position of the phenol motif.¹³³ All synthesized complexes were catalytically active for water oxidation reaction and had a sufficiently low redox potential to permit water oxidation to be driven by [Ru(bpy)₃]³⁺ at neutral reaction conditions. Among the studied WOCs, complex **94** bearing a long alkyl chain with a terminal carboxylate group exposed a higher activity towards H₂O oxidation reaction. Surprisingly, the better performance of **94** was due to the pre-orientation of the incoming H₂O nucleophile as well as H-bonding between a high-valent Mn-oxo/hydroxy group and the distal carboxylate group. This H-bonded scaffold assisted water oxidation reaction by promoting the PCET processes.

11. Manganese complexes as catalyst precursors for water oxidation:

The OEC (oxygen evolving complex) of PSII is composed of four Mn atoms. Inspired by this, scientists have developed a good number of tetranuclear Mn clusters. Dismukes *et al.* prepared a tetranuclear Mn-oxo cubane core [Mn₄O₄L₆]⁺ {where L = (*p*-MeO-C₆H₄)₂PO₂⁻} using phenylphosphonic acid as template. This manganese cluster produced one mole of O₂ per mole of tetranuclear core in the presence of visible light.¹³⁴⁻¹³⁶ Spiccia *et al.* applied [Mn₄O₄L₆]⁺ manganese-oxo cubane catalysts suspended within Nafion membrane for photo-electrochemical water splitting (Figure 34).¹³⁷⁻¹⁴⁰ Without any external bias, this system was able to perform oxidation of H₂O to molecular O₂ in the presence of visible light. EPR and electrochemical studies concluded that the Mn cubane structure was unchanged during catalytic reactions.^{141, 142}

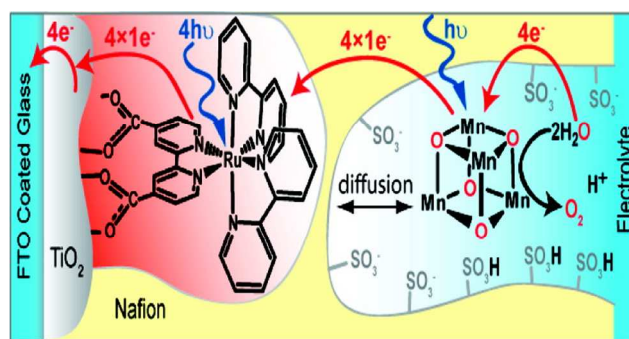


Figure 34 Schematic representation of photo-electrochemical cell where the tetranuclear Mn cubane, [Mn₄O₄L₆]⁺ was used as water oxidation catalyst.

In contrast, during bulk electrolysis experiment using the same catalyst, a reddish brown solid was formed generating a white cloudy solution.¹⁴³ The UV-Vis spectra of this solution exhibited only the absorption maxima at ~230 nm responsible for the ligand, suggesting that tetranuclear Mn-oxo cubane core $[\text{Mn}_4\text{O}_4\text{L}_6]^+$ decomposed during bulk electrolysis. The formed reddish brown solid during the course of bulk electrolysis was insoluble in aqueous and organic solvents and was proposed to be nanostructured MnO_x . Furthermore, XAS measurements of $[\text{Mn}_4\text{O}_4\text{L}_6]^+$ in acetonitrile and $[\text{Mn}_4\text{O}_4\text{L}_6]^+$ loaded into Nafion membrane for comparison were carried out. A significant shift of XANES (X-ray absorption near edge structure) signal to a lower energy was discovered for $[\text{Mn}_4\text{O}_4\text{L}_6]^+$ loaded into Nafion. The energy of this new peak was very logical with the reduction of $[\text{Mn}_4\text{O}_4\text{L}_6]^+$ to Mn(II) species. Water oxidation catalysis using $[(\text{bpy})_2\text{Mn}(\text{O})_2\text{Mn}(\text{bpy})_2]$ ($\text{bpy}=2,2'$ -bipyridine) and Mn^{2+} doped in Nafion membrane to prove that $[\text{Mn}_4\text{O}_4\text{L}_6]^+$ in Nafion was only a precursor for the active catalytic material were done. The photocurrent obtained from the catalytic water oxidation at 1.0V vs Ag/AgCl by $[\text{Mn}_4\text{O}_4\text{L}_6]^+$, $[(\text{bpy})_2\text{Mn}(\text{O})_2\text{Mn}(\text{bpy})_2]$ and Mn^{2+} doped in Nafion were similar, confirming that all the manganese catalysts produced the same species during oxidation in Nafion. So, upon deep investigation it was confirmed that nanostructured manganese oxide phase *e.g.* birnessite oxide lattice, which are true catalytically active species were formed *in-situ* during catalysis. These findings suggested that tetranuclear Mn cubane $[\text{Mn}_4\text{O}_4\text{L}_6]^+$ only acted as a precursor to the catalytically active nanostructured substances.

Complex **95** adsorbed into kaolin clay worked as heterogeneous phase catalyst for the oxidation of water.¹⁴⁴ The water oxidation reaction using **95** was performed in the presence of Ce(IV). No O_2 was produced when only homogeneous **95** was applied as catalyst for the oxidation reaction but when **95** adsorbed into kaolin clay was used as catalyst, significant O_2 evolution was observed. The amount of O_2 produced from this system built up over increasing concentration of **95** in kaolin clay, suggesting that **95** adsorbed into kaolin decomposed during catalysis. In 2012, Moghaddam *et al.* proved that nanoparticles were formed during the reaction between manganese complexes, **95-97** and cerium(IV) ammonium nitrate and these nanoparticles were proposed as active catalysts for water oxidation.¹⁴⁵ All the manganese complexes, **95-97** investigated in their study decomposed in the presence of Ce(IV) to produce a brown coloured solution which gave a solid after evaporation. IR of the solid product confirmed the absence of organic groups and therefore, it was suggested that $\text{Mn}(\text{H}_2\text{O})_6^{3+}$ ions were formed by the decomposition reaction of Ce(IV) and manganese complexes. CO_2 evolution was detected during reaction of manganese complexes with Ce(IV) due to the ligand oxidation. The solutions after titration of all manganese complexes and $\text{Mn}(\text{H}_2\text{O})_6^{2+}$ with Ce(IV) showed similar UV-Vis spectra. Studies of the brown solid using FTIR, XPS, TEM, SEM, XRD, TEM and SEM analyses showed the presence of nanoparticles. FTIR spectra of solid revealed a sharp adsorption peak in the region $400\text{-}500\text{cm}^{-1}$ assigned to the stretching vibration of the Mn-O bond. XPS analysis confirmed that the surface of the solid was mainly composed of Mn and O. **95**-clay hybrid was treated with ~0.2M solution of Ce(IV) and it was observed that the surface of the

compound was mainly composed of Mn and O by XPS. FTIR and XRD also confirmed the presence MnO_2 and MnO in the hybrid compound. Furthermore, it was demonstrated that MnO_2 -clay hybrid in the presence of Ce(IV) was the active catalyst for water oxidation.

In 2013, Spiccia *et al.* reported that manganese oxide nanoparticles were produced *in-situ* in Nafion polymer from **98** and **99** and these nanoparticles were the true and active catalysts for water oxidation.¹⁴⁶ Water oxidation catalysis occurred at 150mV overpotential under neutral reaction media (pH 6.5). X-ray absorption and EPR studies confirmed that the produced material from **98** and **99** in Nafion was in both cases manganese oxide nanoparticles. Transmission electron microscopy measurements of the particles originated from **98** and **99** revealed that MnO_x nanoparticles size range between 10-20 nm for **98** and between 6-10 nm for **99** respectively. A TOF of more than 100 was achieved using 10 nm MnO_x nanoparticles.

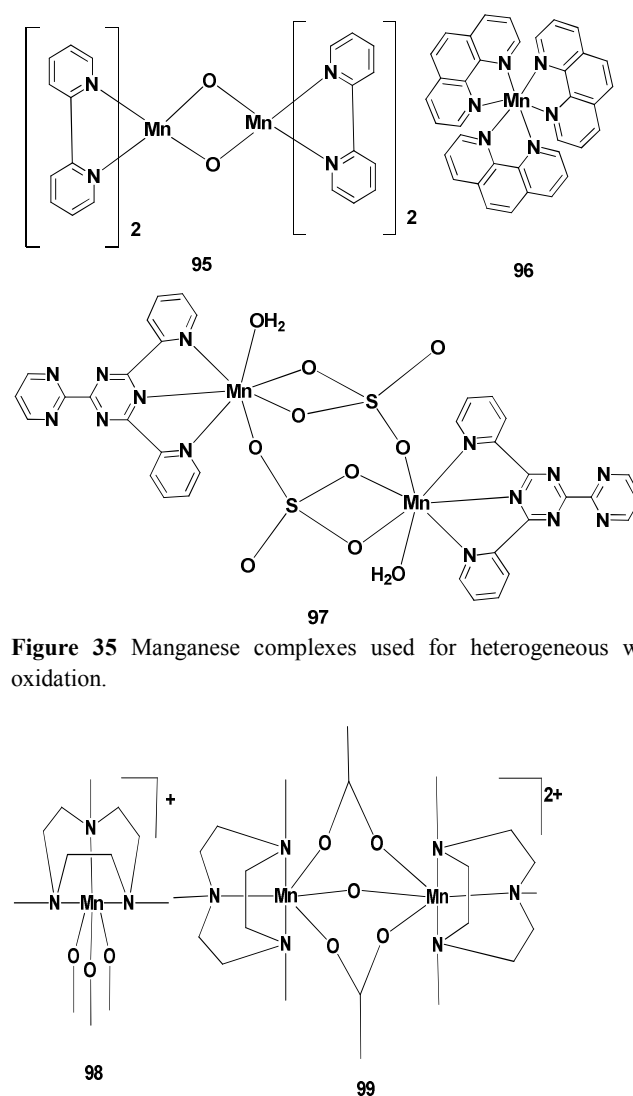


Figure 35 Manganese complexes used for heterogeneous water oxidation.

Figure 36 Molecular structures of $[\text{Mn}(\text{Me}_3\text{TACN})(\text{OMe})_3]^+$, **98** and $[(\text{Me}_3\text{TACN})_2\text{Mn}^{\text{III}}_2(\mu\text{-O})(\mu\text{-CH}_3\text{COO})_2]^{2+}$, **99** where $(\text{Me}_3\text{TACN}) = \text{N},\text{N}',\text{N}'\text{-trimethyl-1,4,7-triazacyclononane}$.

Since proving the homogeneity of catalytic water oxidation processes is a very challenging task, scientists should address the issues of the conversion of homogeneous catalysts into heterogeneous catalysts when manganese catalysts are used. Built on the available data, the strategy of using Mn₂-compounds looks unlikely to succeed, because none of the complexes reported so far meets all of the major requirements that seem mandatory for the catalytic reaction. A successful manganese water-oxidation catalyst is expected to possess an oxidation stable, multinuclear manganese-oxido core, allowing the removal of four electrons at potentials > +1 V in one-electron oxidation steps. In addition, the catalyst is supposed to level the potentials of the different oxidation steps through ligand exchange and/or proton-coupled electron-transfer processes. The multi-nuclear compound should be held together by a rather flexible ligand framework in order to react to the necessary oxidation- and ligand-exchange-events by changes in geometry, and most importantly to have vacant coordination sites for the H₂O substrate. Manganese complexes containing a noninnocent distal group in the ligand frameworks did not receive much attention in water oxidation catalysis and might be a useful approach for promoting catalytic oxidation of H₂O.

As delineate higher, several molecular complexes of earth-abundant metals are often modified to provide metal hydroxide or oxide nanoparticles that could be active catalysts for the oxidation reaction of water. In some examples of chemical and light-driven water-oxidation reaction, CO₂ gas was produced with the evolution of O₂ because of the oxidation of ligands. GC and MS techniques are the most reliable techniques for the quantification and identification of O₂ produced during water-oxidation catalysis, whereas methods such as electrode probes and manometry are expected to be avoided for O₂ quantification. CO₂ gas formation due to ligand oxidation occurring during water-oxidation catalysis cannot be separated by the technique of manometry and powerful acidic environments might have an effect on the probe. Since metal ions leach from the complexes and may produce nanoparticles, the water oxidation activity of the homogeneous metal catalysts ought to be examined with its nanoparticles to be a proof of homogenous catalysis. Occasionally, each homogenous and heterogeneous form may exist alone in the reaction media. Furthermore, reactive materials can be modified throughout the oxidation process. So, analytical studies for the detection of the real catalyst for water oxidation reaction must be carried out adequately.

12. Conclusions:

Complexes of earth-abundant metals can act as catalysts or precatalysts for water oxidation reaction. Molecular metal complexes as catalysts are either homogeneous or heterogeneous during water oxidation catalysis depending on the sort of metals, pH, oxidants, and supporting ligands. The organic ligands of Co-complexes were additionally oxidized throughout the light-driven water oxidation reaction in neutral and basic media by [Ru(bpy)₃]²⁺/S₂O₈²⁻ system to provide cobalt hydroxide nanoparticles that worked as the true catalysts for water oxidation reaction. Some of the molecular Fe-complexes work as homogeneous catalysts in water oxidation

reaction with ceric ammonium nitrate (CAN) as oxidant in acidic media, though the life-time of the catalysts were short. There are some other Fe-complexes that converted into iron oxide nanoparticles in light-driven water oxidation by [Ru(bpy)₃]²⁺ with Na₂S₂O₈ under basic reaction conditions and performed as real catalysts for the catalytic water oxidation reaction. There are limited reports about the exploration of nickel complexes for the water-oxidation reaction in a catalytic system. Till now, there is a single report on a homogeneous nickel complex within the literature as WOCs. On the other hand, nickel complexes generally form nanoparticles in basic conditions and act as real catalysts for water-oxidation reaction. Molecular complexes of copper act as homogeneous or heterogeneous catalyst depending on the supporting ligands and pH scale. Manganese complexes also can act as homogeneous and heterogeneous catalyst for water oxidation reaction depending on the reaction conditions. Particularly, strong acidic/basic reaction media or oxidizing/reducing reaction conditions favour the decomposition of manganese complexes into MnO_x nanoparticles. Not exclusively the selection of metal and supporting ligands but also the reaction conditions (pH and oxidants) play a vital role in resolving the water oxidation activity of the catalysts in each homogeneous and heterogeneous medium. Though the starting metal catalysts (metal complexes) are homogeneous, it is attainable that they can regenerate metal oxide or hydroxide nanoparticles during water oxidation catalysis and can act as true catalysts and therefore, these phenomena should be examined carefully.

A complete set of characterization techniques should be carried out to prove the stability of the starting complex under turnover conditions. It is very important to carefully characterize the active species, before, during and after water oxidation catalysis by various spectroscopic methods, microscopic methods and DLS measurements for concluding whether the catalytic process is homogeneous or heterogeneous. Metal complexes synthesized as homogeneous WOCs are normally characterized crystallographically. EPR and XAS spectroscopies can be used to know more about electronic and nuclear structural information of WOCs. XPS spectroscopy can give clear information about different elements present in the post photo/electrolysis products and their respective oxidation states that can be clearly compared with the starting metal complexes. This might give an indication about structure conformations or decomposition. Moreover, EDX spectroscopy can be used for elemental analysis and chemical characterization of a definite surface. To characterize and visualize the electrode used for water oxidation reaction, scanning electron microscopy (SEM) is a well-known technique but it needs deposition of materials on the surface of electrode. TEM can be used to visualize nanometer and subnanometer particles formed during catalytic reaction. Finally, dynamic light scattering (DLS) is a reliable technique for detecting the presence or absence of nanoparticles in solution. However, care much be taken and combined analysis should be considered before one can claim a homo/heterogeneous process. If each of the measurements give positive results then only it is possible to conclude about the stability of initial complex or about the nature of the true catalytic species in water oxidation catalysis where a metal complex is used as catalyst

(or precatalyst). In light of the speedily growing demand for economical and robust water-oxidation catalysts, the collaborations between researchers in the fields of homogeneous and heterogeneous water-oxidation catalysis can promisingly accelerate their research towards sensible applications of water-oxidation catalysts.

Acknowledgements

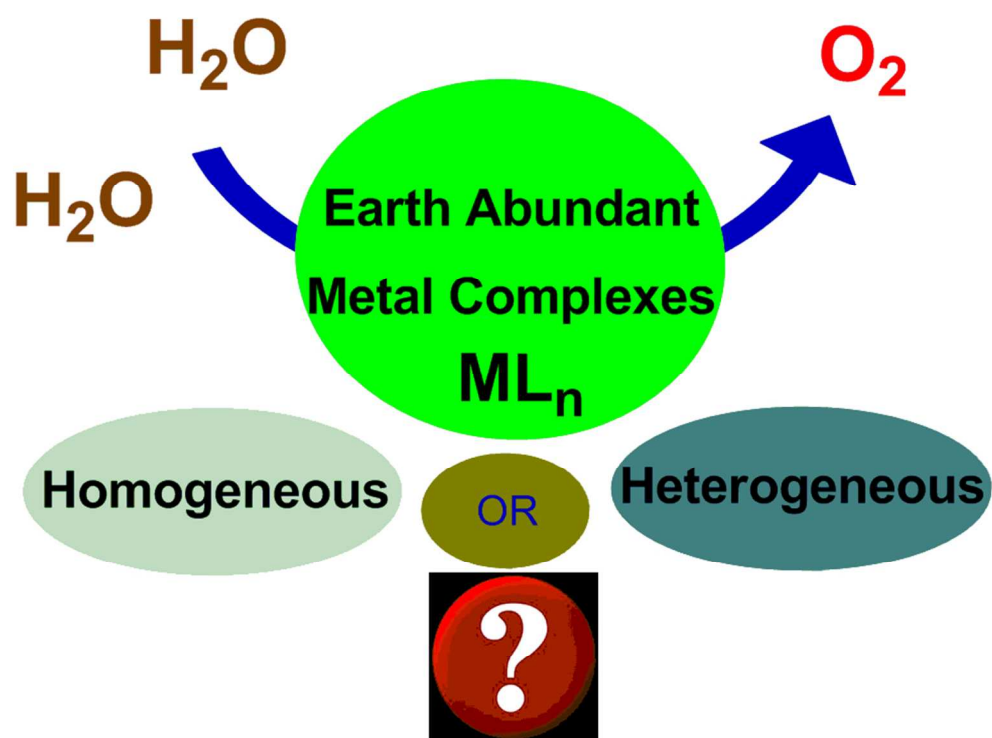
The authors would like to express their deep accolade to “State Key Lab of Advanced Technology for Materials Synthesis and Processing” for financial support. F.V. acknowledges the Chinese Central Government for an “Expert of the State” position in the program of “Thousand Talent” as well as the support of the National Science Foundation China (No. 21172027). M.A.A. and H.A.Y. acknowledge the Chinese Scholarship Council (CSC) for their PhD grants 2013GXZ983 and 2012GXZ63.

Notes and references

- H. B. Gray, *Nat. Chem.*, 2009, **1**, 7-7.
- D. L. Royer, R. A. Berner and J. Park, *Nature*, 2007, **446**, 530-532.
- N. S. Lewis and D. G. Nocera, *Proc. Natl. Acad. Sci.*, 2006, **103**, 15729-15735.
- S. Fukuzumi, *Eur. J. Inorg. Chem.*, 2008, **2008**, 1351-1362.
- V. Balzani, A. Credi and M. Venturi, *ChemSusChem*, 2008, **1**, 26-58.
- T. R. Cook, D. K. Dogutan, S. Y. Reece, Y. Surendranath, T. S. Teets and D. G. Nocera, *Chem. Rev.*, 2010, **110**, 6474-6502.
- D. G. Nocera, *Acc. Chem. Res.*, 2012, **45**, 767-776.
- S. Fukuzumi, *Phys. Chem. Chem. Phys.*, 2008, **10**, 2283-2297.
- D. Gust, T. A. Moore and A. L. Moore, *Acc. Chem. Res.*, 2009, **42**, 1890-1898.
- S. Fukuzumi and T. Kojima, *J. Mater. Chem.*, 2008, **18**, 1427-1439.
- S. Fukuzumi and K. Ohkubo, *J. Mater. Chem.*, 2012, **22**, 4575-4587.
- J. J. Concepcion, R. L. House, J. M. Papanikolas and T. J. Meyer, *Proc. Natl. Acad. Sci.*, 2012, **109**, 15560-15564.
- M. R. Wasielewski, *Acc. Chem. Res.*, 2009, **42**, 1910-1921.
- P. D. Frischmann, K. Mahata and F. Würthner, *Chem. Soc. Rev.*, 2013, **42**, 1847-1870.
- D. Gust, T. A. Moore and A. L. Moore, *Acc. Chem. Res.*, 2001, **34**, 40-48.
- M. N. Paddon-Row, *Proc. Natl. Acad. Sci.*, 2003, **38**, 1-85.
- M. R. Wasielewski, *Chem. Rev.*, 1992, **92**, 435-461.
- S. Fukuzumi, Y. Yamada, T. Suenobu, K. Ohkubo and H. Kotani, *Energy Environ. Sci.*, 2011, **4**, 2754-2766.
- M. Rudolf, S. Wolfrum, D. M. Guldi, L. Feng, T. Tsuchiya, T. Akasaka and L. Echegoyen, *Chem. Eur. J.*, 2012, **18**, 5136-5148.
- D. M. Guldi, G. A. Rahman, V. Sgobba and C. Ehli, *Chem. Soc. Rev.*, 2006, **35**, 471-487.
- G. Bottari, G. de la Torre, D. M. Guldi and T. Torres, *Chem. Rev.*, 2010, **110**, 6768-6816.
- S. Fukuzumi, *Bull. Chem. Soc. Jpn.*, 2006, **79**, 177-195.
- F. D'Souza and O. Ito, *Chem. Soc. Rev.*, 2012, **41**, 86-96.
- F. D'Souza and O. Ito, *Chem. Commun.*, 2009, 4913-4928.
- R. Chitta and F. D'Souza, *J. Mater. Chem.*, 2008, **18**, 1440-1471.
- H. Kotani, R. Hanazaki, K. Ohkubo, Y. Yamada and S. Fukuzumi, *Chem. Eur. J.*, 2011, **17**, 2777-2785.
- Y. Yamada, T. Miyahigashi, H. Kotani, K. Ohkubo and S. Fukuzumi, *J. Am. Chem. Soc.*, 2011, **133**, 16136-16145.
- Y. Yamada, T. Miyahigashi, H. Kotani, K. Ohkubo and S. Fukuzumi, *Energy Environ. Sci.*, 2012, **5**, 6111-6118.
- B. Mondal, K. Sengupta, A. Rana, A. Mahammed, M. Botoshansky, S. G. Dey, Z. Gross and A. Dey, *Inorg. Chem.*, 2013, **52**, 3381-3387.
- M. J. Rose, H. B. Gray and J. R. Winkler, *J. Am. Chem. Soc.*, 2012, **134**, 8310-8313.
- T. M. McCormick, Z. Han, D. J. Weinberg, W. W. Brennessel, P. L. Holland and R. Eisenberg, *Inorg. Chem.*, 2011, **50**, 10660-10666.
- Z. Han, W. R. McNamara, M.-S. Eum, P. L. Holland and R. Eisenberg, *Angew. Chem.*, 2012, **124**, 1699-1702.
- H. I. Karunadasa, C. J. Chang and J. R. Long, *Nature*, 2010, **464**, 1329-1333.
- H. I. Karunadasa, E. Montalvo, Y. Sun, M. Majda, J. R. Long and C. J. Chang, *Science*, 2012, **335**, 698-702.
- A. E. King, Y. Surendranath, N. A. Piro, J. P. Bigi, J. R. Long and C. J. Chang, *Chem. Sci.*, 2013, **4**, 1578-1587.
- V. S. Thoi, Y. Sun, J. R. Long and C. J. Chang, *Chem. Soc. Rev.*, 2013, **42**, 2388-2400.
- E. J. Sundstrom, X. Yang, V. S. Thoi, H. I. Karunadasa, C. J. Chang, J. R. Long and M. Head-Gordon, *J. Am. Chem. Soc.*, 2012, **134**, 5233-5242.
- Y. Sun, J. P. Bigi, N. A. Piro, M. L. Tang, J. R. Long and C. J. Chang, *J. Am. Chem. Soc.*, 2011, **133**, 9212-9215.
- X. Li, M. Wang, D. Zheng, K. Han, J. Dong and L. Sun, *Energy Environ. Sci.*, 2012, **5**, 8220-8224.
- L. Chen, M. Wang, F. Gloaguen, D. Zheng, P. Zhang and L. Sun, *Inorg. Chem.*, 2013, **52**, 1798-1806.
- J. Dong, M. Wang, X. Li, L. Chen, Y. He and L. Sun, *ChemSusChem*, 2012, **5**, 2133-2138.
- S. Fukuzumi and T. Suenobu, *Dalton Trans.*, 2013, **42**, 18-28.
- Y. Maenaka, T. Suenobu and S. Fukuzumi, *Energy Environ. Sci.*, 2012, **5**, 7360-7367.
- E. Fujita, J. T. Muckerman and Y. Himeda, *Biochim. Biophys. Acta-Bioenerg.*, 2013, **1827**, 1031-1038.
- W.-H. Wang, J. F. Hull, J. T. Muckerman, E. Fujita and Y. Himeda, *Energy Environ. Sci.*, 2012, **5**, 7923-7926.
- J. F. Hull, Y. Himeda, W.-H. Wang, B. Hashiguchi, R. Periana, D. J. Szalda, J. T. Muckerman and E. Fujita, *Nat Chem*, 2012, **4**, 383-388.
- N. Cox, D. A. Pantazis, F. Neese and W. Lubitz, *Acc. Chem. Res.*, 2013, **46**, 1588-1596.
- Y. Umena, K. Kawakami, J.-R. Shen and N. Kamiya, *Nature*, 2011, **473**, 55-60.
- R. J. Pace, R. Stranger and S. Petrie, *Dalton Trans.*, 2012, **41**, 7179-7189.
- M. M. Najafpour, T. Ehrenberg, M. Wiechen and P. Kurz, *Angew. Chem.*, 2010, **122**, 2281-2285.
- P. E. Siegbahn, *Acc. Chem. Res.*, 2009, **42**, 1871-1880.
- X. Liu and F. Wang, *Coord. Chem. Rev.*, 2012, **256**, 1115-1136.
- A. Sartorel, M. Bonchio, S. Campagna and F. Scandola, *Chem. Soc. Rev.*, 2013, **42**, 2262-2280.
- C. J. Gagliardi, A. K. Vannucci, J. J. Concepcion, Z. Chen and T. J. Meyer, *Energy Environ. Sci.*, 2012, **5**, 7704-7717.
- D. G. Hettterscheid and J. N. Reek, *Angew. Chem.*, 2012, **124**, 9878-9885.
- K. S. Joya, J. L. Vallés-Pardo, Y. F. Joya, T. Eisenmayer, B. Thomas, F. Buda and H. J. de Groot, *ChemPlusChem*, 2013, **78**, 35-47.
- F. Puntoriero, A. Sartorel, M. Orlandi, G. La Ganga, S. Serroni, M. Bonchio, F. Scandola and S. Campagna, *Coord. Chem. Rev.*, 2011, **255**, 2594-2601.
- H. Lv, Y. V. Geletii, C. Zhao, J. W. Vickers, G. Zhu, Z. Luo, J. Song, T. Lian, D. G. Musaev and C. L. Hill, *Chem. Soc. Rev.*, 2012, **41**, 7572-7589.
- A. R. Parent, R. H. Crabtree and G. W. Brudvig, *Chem. Soc. Rev.*, 2013, **42**, 2247-2252.
- D. J. Wasylenko, R. D. Palmer and C. P. Berlinguette, *Chem. Commun.*, 2013, **49**, 218-227.
- R. Cao, W. Lai and P. Du, *Energy Environ. Sci.*, 2012, **5**, 8134-8157.
- S. Fukuzumi and Y. Yamada, *J. Mater. Chem.*, 2012, **22**, 24284-24296.
- M. Yagi and M. Kaneko, *Chem. Rev.*, 2001, **101**, 21-36.
- A. Harriman, I. J. Pickering, J. M. Thomas and P. A. Christensen, *Chem. Soc. Faraday Trans. 1*, 1988, **84**, 2795-2806.
- F. Jiao and H. Frei, *Angew. Chem.*, 2009, **121**, 1873-1876.

66. F. Jiao and H. Frei, *Energy Environ. Sci.*, 2010, **3**, 1018-1027.
67. A. Izgorodin, O. Winther-Jensen and D. R. MacFarlane, *Aust. J. Chem.*, 2012, **65**, 638-642.
68. W. Ostwald, *Nature*, 1902, **65**, 522-526.
69. Y. Lin and R. G. Finke, *Inorg. Chem.*, 1994, **33**, 4891-4910.
70. J. A. Widegren and R. G. Finke, *J. Mol. Catal. A: Chem.*, 2003, **198**, 317-341.
71. X. Sala, I. Romero, M. Rodríguez, L. Escriche and A. Llobet, *Angew. Chem. Int. Ed.*, 2009, **48**, 2842-2852.
72. V. Artero and M. Fontecave, *Chem. Soc. Rev.*, 2013, **42**, 2338-2356.
73. R. H. Crabtree, *Chem. Rev.*, 2011, **112**, 1536-1554.
74. B. Limburg, E. Bouwman and S. Bonnet, *Coord. Chem. Rev.*, 2012, **256**, 1451-1467.
75. J. J. Stracke and R. G. Finke, *ACS Catal.*, 2014, **4**, 909-933.
76. S. Fukuzumi and D. Hong, *Eur. J. Inorg. Chem.*, 2014, **2014**, 645-659.
77. E. Pizzolato, M. Natali, B. Posocco, A. M. López, I. Bazzan, M. Di Valentin, P. Galloni, V. Conte, M. Bonchio and F. Scandola, *Chem. Commun.*, 2013, **49**, 9941-9943.
78. C.-F. Leung, S.-M. Ng, C.-C. Ko, W.-L. Man, J. Wu, L. Chen and T.-C. Lau, *Energy Environ. Sci.*, 2012, **5**, 7903-7907.
79. T. Nakazono, A. R. Parent and K. Sakai, *Chem. Commun.*, 2013, **49**, 6325-6327.
80. D. Wang and J. T. Groves, *Proc. Natl. Acad. Sci.*, 2013, **110**, 15579-15584.
81. D. J. Wasylenko, C. Ganesamoorthy, J. Borau-Garcia and C. P. Berlinguette, *Chem. Commun.*, 2011, **47**, 4249-4251.
82. R. McGuire Jr, D. K. Dogutan, T. S. Teets, J. Suntivich, Y. Shao-Horn and D. G. Nocera, *Chem. Sci.*, 2010, **1**, 411-414.
83. D. K. Dogutan, R. McGuire Jr and D. G. Nocera, *J. Am. Chem. Soc.*, 2011, **133**, 9178-9180.
84. H. Wang, Y. Lu, E. Mijangos and A. Thapper, *Chin. J. Chem.*, 2014, **32**, 467-473.
85. M. L. Rigsby, S. Mandal, W. Nam, L. C. Spencer, A. Llobet and S. S. Stahl, *Chem. Sci.*, 2012, **3**, 3058-3062.
86. H. Chen, Z. Sun, X. Liu, A. Han and P. Du, *J. Phys. Chem. C*, 2015, **119**, 8998-9004.
87. S. Fu, Y. Liu, Y. Ding, X. Du, F. Song, R. Xiang and B. Ma, *Chem. Commun.*, 2014, **50**, 2167-2169.
88. D. Hong, J. Jung, J. Park, Y. Yamada, T. Suenobu, Y.-M. Lee, W. Nam and S. Fukuzumi, *Energy Environ. Sci.*, 2012, **5**, 7606-7616.
89. N. S. McCool, D. M. Robinson, J. E. Sheats and G. C. Dismukes, *J. Am. Chem. Soc.*, 2011, **133**, 11446-11449.
90. S. Berardi, G. La Ganga, M. Natali, I. Bazzan, F. Puntoriero, A. Sartorel, F. Scandola, S. Campagna and M. Bonchio, *J. Am. Chem. Soc.*, 2012, **134**, 11104-11107.
91. A. M. Ullman, Y. Liu, M. Huynh, D. K. Bediako, H. Wang, B. L. Anderson, D. C. Powers, J. J. Breen, H. D. Abruña and D. G. Nocera, *J. Am. Chem. Soc.*, 2014, **136**, 17681-17688.
92. W. C. Ellis, N. D. McDaniel, S. Bernhard and T. J. Collins, *J. Am. Chem. Soc.*, 2010, **132**, 10990-10991.
93. J. L. Fillol, Z. Codolà, I. Garcia-Bosch, L. Gómez, J. J. Pla and M. Costas, *Nat. Chem.*, 2011, **3**, 807-813.
94. Z. Codolà, I. Garcia-Bosch, F. Acuña-Parés, I. Prat, J. M. Luis, M. Costas and J. Lloret-Fillol, *Chem. Eur. J.*, 2013, **19**, 8042-8047.
95. B. Zhang, F. Li, F. Yu, H. Cui, X. Zhou, H. Li, Y. Wang and L. Sun, *Chem. Asian J.*, 2014, **9**, 1515-1518.
96. M. K. Coggins, M.-T. Zhang, A. K. Vannucci, C. J. Dares and T. J. Meyer, *J. Am. Chem. Soc.*, 2014, **136**, 5531-5534.
97. D. Hong, S. Mandal, Y. Yamada, Y.-M. Lee, W. Nam, A. Llobet and S. Fukuzumi, *Inorg. Chem.*, 2013, **52**, 9522-9531.
98. W. A. Hoffert, M. T. Mock, A. M. Appel and J. Y. Yang, *Eur. J. Inorg. Chem.*, 2013, **2013**, 3846-3857.
99. G. Chen, L. Chen, S. M. Ng, W. L. Man and T. C. Lau, *Angew. Chem. Int. Ed.*, 2013, **52**, 1789-1791.
100. M. Zhang, M.-T. Zhang, C. Hou, Z.-F. Ke and T.-B. Lu, *Angew. Chem. Int. Ed.*, 2014, **53**, 13042-13048.
101. G. Chen, L. Chen, S. M. Ng and T. C. Lau, *ChemSusChem*, 2014, **7**, 127-134.
102. A. Singh, S. L. Chang, R. K. Hocking, U. Bach and L. Spiccia, *Catal. Sci. Technol.*, 2013, **3**, 1725-1732.
103. A. Singh, S. L. Chang, R. K. Hocking, U. Bach and L. Spiccia, *Energy Environ. Sci.*, 2013, **6**, 579-586.
104. S. M. Barnett, K. I. Goldberg and J. M. Mayer, *Nat. Chem.*, 2012, **4**, 498-502.
105. M.-T. Zhang, Z. Chen, P. Kang and T. J. Meyer, *J. Am. Chem. Soc.*, 2013, **135**, 2048-2051.
106. L.-L. Zhou, T. Fang, J.-P. Cao, Z.-H. Zhu, X.-T. Su and S.-Z. Zhan, *J. Power Sources*, 2015, **273**, 298-304.
107. W.-B. Yu, Q.-Y. He, X.-F. Ma, H.-T. Shi and X. Wei, *Dalton Trans.*, 2015, **44**, 351-358.
108. X. Liu, H. Jia, Z. Sun, H. Chen, P. Xu and P. Du, *Electrochem. Commun.*, 2014, **46**, 1-4.
109. Y. Naruta, M. a. Sasayama and T. Sasaki, *Angew. Chem., Int. Ed. Engl.*, 1994, **33**, 1839-1841.
110. J. Limburg, J. S. Vrettos, L. M. Liable-Sands, A. L. Rheingold, R. H. Crabtree and G. W. Brudvig, *Science*, 1999, **283**, 1524-1527.
111. J. Limburg, J. S. Vrettos, H. Chen, J. C. de Paula, R. H. Crabtree and G. W. Brudvig, *J. Am. Chem. Soc.*, 2001, **123**, 423-430.
112. C. W. Cady, K. E. Shinopoulos, R. H. Crabtree and G. W. Brudvig, *Dalton Trans.*, 2010, **39**, 3985-3989.
113. H. Chen, R. Tagore, S. Das, C. Incarvito, J. Faller, R. H. Crabtree and G. W. Brudvig, *Inorg. Chem.*, 2005, **44**, 7661-7670.
114. H. Yamazaki, S. Igarashi, T. Nagata and M. Yagi, *Inorg. Chem.*, 2012, **51**, 1530-1539.
115. H. Chen, R. Tagore, G. Olack, J. S. Vrettos, T.-C. Weng, J. Penner-Hahn, R. H. Crabtree and G. W. Brudvig, *Inorg. Chem.*, 2007, **46**, 34-43.
116. R. Tagore, R. H. Crabtree and G. W. Brudvig, *Inorg. Chem.*, 2008, **47**, 1815-1823.
117. J. Limburg, G. W. Brudvig and R. H. Crabtree, *J. Am. Chem. Soc.*, 1997, **119**, 2761-2762.
118. R. Tagore, H. Chen, H. Zhang, R. H. Crabtree and G. W. Brudvig, *Inorg. Chim. Acta*, 2007, **360**, 2983-2989.
119. P. Kurz, G. Berggren, M. F. Anderlund and S. Styring, *Dalton Trans.*, 2007, 4258-4261.
120. C. Baffert, S. Romain, A. Richardot, J.-C. Leprêtre, B. Lefebvre, A. Deronzier and M.-N. Collomb, *J. Am. Chem. Soc.*, 2005, **127**, 13694-13704.
121. M. Yagi and K. Narita, *J. Am. Chem. Soc.*, 2004, **126**, 8084-8085.
122. H. Chen, J. Faller, R. H. Crabtree and G. W. Brudvig, *J. Am. Chem. Soc.*, 2004, **126**, 7345-7349.
123. H. Chen, M.-N. Collomb, C. Duboc, G. Blondin, E. Rivière, J. Faller, R. H. Crabtree and G. W. Brudvig, *Inorg. Chem.*, 2005, **44**, 9567-9573.
124. Y. Gao, R. H. Crabtree and G. W. Brudvig, *Inorg. Chem.*, 2012, **51**, 4043-4050.
125. A. K. Poulsen, A. Rompel and C. J. McKenzie, *Angew. Chem. Int. Ed.*, 2005, **44**, 6916-6920.
126. R. K. Seidler-Egdal, A. Nielsen, A. D. Bond, M. J. Bjerrum and C. J. McKenzie, *Dalton Trans.*, 2011, **40**, 3849-3858.
127. G. Berggren, A. Thapper, P. Huang, P. Kurz, L. Eriksson, S. Styring and M. F. Anderlund, *Dalton Trans.*, 2009, 10044-10054.
128. G. Berggren, A. Thapper, P. Huang, L. Eriksson, S. r. Styring and M. F. Anderlund, *Inorg. Chem.*, 2011, **50**, 3425-3430.
129. K. J. Young, M. K. Takase and G. W. Brudvig, *Inorg. Chem.*, 2013, **52**, 7615-7622.
130. Y. Gao, J. Liu, M. Wang, Y. Na, B. Åkermark and L. Sun, *Tetrahedron*, 2007, **63**, 1987-1994.
131. Y. Gao, T. r. Åkermark, J. Liu, L. Sun and B. r. Åkermark, *J. Am. Chem. Soc.*, 2009, **131**, 8726-8727.
132. E. A. Karlsson, B.-L. Lee, T. Åkermark, E. V. Johnston, M. D. Kärkäs, J. Sun, Ö. Hansson, J.-E. Bäckvall and B. Åkermark, *Angew. Chem. Int. Ed.*, 2011, **50**, 11715-11718.
133. W. A. Arafat, M. D. Kärkäs, B.-L. Lee, T. Åkermark, R.-Z. Liao, H.-M. Berends, J. Messinger, P. E. Siegbahn and B. Åkermark, *Phys. Chem. Chem. Phys.*, 2014, **16**, 11950-11964.
134. W. Ruettinger, M. Yagi, K. Wolf, S. Bernasek and G. Dismukes, *J. Am. Chem. Soc.*, 2000, **122**, 10353-10357.
135. J.-Z. Wu, F. De Angelis, T. G. Carrell, G. P. Yap, J. Sheats, R. Car and G. C. Dismukes, *Inorg. Chem.*, 2006, **45**, 189-195.
136. C. W. Cady, R. H. Crabtree and G. W. Brudvig, *Coord. Chem. Rev.*, 2008, **252**, 444-455.

137. R. Brimblecombe, G. F. Swiegers, G. C. Dismukes and L. Spiccia, *Angew. Chem. Int. Ed.*, 2008, **47**, 7335-7338.
138. R. Brimblecombe, A. Koo, G. C. Dismukes, G. F. Swiegers and L. Spiccia, *J. Am. Chem. Soc.*, 2010, **132**, 2892-2894.
139. R. Brimblecombe, A. Koo, G. C. Dismukes, G. F. Swiegers and L. Spiccia, *ChemSusChem*, 2010, **3**, 1146-1150.
140. G. C. Dismukes, R. Brimblecombe, G. A. Felton, R. S. Pryadun, J. E. Sheats, L. Spiccia and G. F. Swiegers, *Acc. Chem. Res.*, 2009, **42**, 1935-1943.
141. R. Brimblecombe, D. R. Kolling, A. M. Bond, G. C. Dismukes, G. F. Swiegers and L. Spiccia, *Inorg. Chem.*, 2009, **48**, 7269-7279.
142. R. Brimblecombe, A. M. Bond, G. C. Dismukes, G. F. Swiegers and L. Spiccia, *Phys. Chem. Chem. Phys.*, 2009, **11**, 6441-6449.
143. R. K. Hocking, R. Brimblecombe, L.-Y. Chang, A. Singh, M. H. Cheah, C. Glover, W. H. Casey and L. Spiccia, *Nat. Chem.*, 2011, **3**, 461-466.
144. R. Ramaraj, A. Kira and M. Kaneko, *Chem. Lett.*, 1987, **16**, 261-264.
145. M. M. Najafpour, F. Rahimi, M. Amini, S. Nayeri and M. Bagherzadeh, *Dalton Trans.*, 2012, **41**, 11026-11031.
146. A. Singh, R. K. Hocking, S. L.-Y. Chang, B. M. George, M. Fehr, K. Lips, A. Schnegg and L. Spiccia, *Chem. Mater.*, 2013, **25**, 1098-1108.



84x63mm (300 x 300 DPI)